Environment International 184 (2024) 108481

Contents lists available at ScienceDirect

Environment International

journal homepage: www.elsevier.com/locate/envint

Full length article

In vitro neurotoxicity of particles from diesel and biodiesel fueled engines following direct and simulated inhalation exposure

Lora-Sophie Gerber [a,b], Dirk C.A. de Leijer [a], Andrea Rujas Arranz [a], Jonas M.M.L. Lehmann [a,b], Meike E. Verheul [a], Flemming R. Cassee [a,b], Remco H.S. Westerink [a,*]

[a] Institute for Risk Assessment Sciences (IRAS), Faculty of Veterinary Medicine, Utrecht University, Utrecht, the Netherlands
[b] National Institute for Public Health and the Environment (RIVM), Bilthoven, the Netherlands

ARTICLE INFO

Keywords:
Air pollution
Diesel engine emission
Neurotoxic hazard characterization
Microelectrode array recordings
Inhalation exposure

ABSTRACT

Combustion-derived particulate matter (PM) is a major source of air pollution. Efforts to reduce diesel engine emission include the application of biodiesel. However, while urban PM exposure has been linked to adverse brain effects, little is known about the direct effects of PM from regular fossil diesel (PMDEP) and biodiesel (PMBIO) on neuronal function. Furthermore, it is unknown to what extent the PM-induced effects in the lung (e.g., inflammation) affect the brain. This *in vitro* study investigates direct and indirect toxicity of PMDEP and PMBIO on the lung and brain and compared it with effects of clean carbon particles (CP).

PM were generated using a common rail diesel engine. CP was sampled from a spark generator. First, effects of 48 h exposure to PM and CP (1.2–3.9 μg/cm^2) were assessed in an *in vitro* lung model (air–liquid interface co-culture of Calu-3 and THP1 cells) by measuring cell viability, cytotoxicity, barrier function, inflammation, and oxidative and cell stress. None of the exposures caused clear adverse effects and only minor changes in gene expression were observed.

Next, the basal medium was collected for subsequent simulated inhalation exposure of rat primary cortical cells. Neuronal activity, recorded using microelectrode arrays (MEA), was increased after acute (0.5 h) simulated inhalation exposure. In contrast, direct exposure to PMDEP and PMBIO (1–100 μg/mL; 1.2–119 μg/cm^2) reduced neuronal activity after 24 h with lowest observed effect levels of respectively 10 μg/mL and 30 μg/mL, indicating higher neurotoxic potency of PMDEP, whereas neuronal activity remained unaffected following CP exposure.

These findings indicate that combustion-derived PM potently inhibit neuronal function following direct exposure, while the lung serves as a protective barrier. Furthermore, PMDEP exhibit a higher direct neurotoxic potency than PMBIO, and the data suggest that the neurotoxic effects is caused by adsorbed chemicals rather than the pure carbon core.

1. Introduction

Air pollution is a complex mixture of gaseous compounds and particular matter (PM), the latter consisting of solid particles and liquid droplets. Scientific evidence supports that chronic exposure to air pollution and ambient PM is not only associated with increased severity of respiratory and cardiovascular diseases, but also with adverse effects on the brain and neurodegenerative diseases (Cacciottolo et al., 2017; Costa et al., 2014; Lucchini et al., 2012; Peters et al., 2019; Costa et al., 2017; Calderón-Garcidueñas and Ayala, 2021).

PM can be distinguished using common cut-off points of the aerodynamic diameter during sampling including 10 μm, 2.5 μm and 0.1 μm, which refers to coarse (PM10), fine (PM2.5), and ultrafine (PM0.1) particles, respectively. PM size is one of the physical key parameters determining particle deposition and thereby the internal dose and fate of the particle following inhalation (Braakhuis et al., 2014; Oberdörster et al., 2009). In particular, the smaller the particles the higher the likelihood that they deposit in the lower respiratory tract, whereas larger inhaled particles are retained by the upper airways, i.e. nasopharyngeal region (Kuempel et al., 2015; Carvalho et al., 2011). Comparable to engineered nanomaterials (<100 nm), PM0.1 can translocate from the alveolar space into the systemic circulation and as a

* Corresponding author at: Neurotoxicology Research Group, Division of Toxicology, Institute for Risk Assessment Sciences (IRAS), Faculty of Veterinary Medicine, Utrecht University, P.O. Box 80.177, NL-3508 TD Utrecht, The Netherlands.
E-mail address: R.Westerink@uu.nl (R.H.S. Westerink).

https://doi.org/10.1016/j.envint.2024.108481
Received 24 November 2023; Received in revised form 17 January 2024; Accepted 2 February 2024
Available online 5 February 2024

consequence can reach secondary target organs including the brain (Kreyling et al., 2016; Miller et al., 2017; Oberdörster et al., 2009, 2004; Bongaerts et al., 2022). Additionally, a considerable fraction of PM0.1 deposits on and accumulates in the olfactory epithelium (Kuempel et al., 2015; Oberdörster et al., 2004) from where it can access the brain directly via diffusion into the olfactory nerves as demonstrated for solid nanomaterials including carbon particles (Elder et al., 2006; Kreyling, 2016; Lucchini et al., 2012; Oberdörster et al., 2004).

A significant part of urban air pollution derives from traffic with combustion particles from diesel engine exhaust being a major source of PM2.5 (Cassee et al., 2013; Karagulian et al., 2015). Compared to gasoline engines, traditional diesel engines emit a larger particle mass and number, and more heterogeneous PM (Donaldson et al., 2005; Ristovski et al., 2012; Schwarze et al., 2013). Consequently, diesel engine exhaust-derived PM has been in the focus of research and policy measures.

Diesel PM is generated due to incomplete combustion and consists of solid particles with a carbonaceous core composed of elemental carbon and volatile particles consisting of semi-volatile organic compounds (SVOC). On the surface of the carbonaceous core, solid particles can adsorb a wide variety of compounds, including combustion-derived compounds such SVOC and metals (Cassee et al., 2013; Omidvarborna et al., 2015). The smaller the particle is, the larger the surface area per unit volume of a particle becomes. Thereby, particles, in particular the smallest fraction (PM0.1), can serve as a carrier that crucially impacts the hazard of diesel PM for the different target organs (Cassee et al., 2013; Schraufnagel, 2020). In the past years, efforts have been made to reduce diesel engine exhaust emission and to alter its composition in an attempt to reduce air pollution and toxic potency of the PM emission amongst others, by modification of the fuel composition including the introduction of biodiesel fuel. However, the impact of replacing petroleum-based diesel with biodiesel fuel on the neurotoxic potency of the emitted PM is yet unknown.

Oxidative stress and inflammation are key mechanisms underlying PM-induced toxicity (Cassee et al., 2013; Ristovski et al., 2012; Schwarze et al., 2013). Inhalation of PM from diesel engines caused local inflammation in the lungs of exposed animals (Ishihara and Kagawa, 2003), as well as systemic inflammation (Upadhyay et al., 2008) and neuroinflammation (Costa et al., 2019; Heusinkveld et al., 2016). Results from *in vivo* studies suggest that systemic inflammation can initiate and promote neuroinflammatory processes, which in turn contributes to the onset and progression of neurodegeneration (Shkirkova et al., 2022; Costa et al., 2019; Heusinkveld et al., 2016). Brains of animals exposed to diesel particles or traffic-derived PM exhibit oxidative damage and upregulated the expression of oxidative stress-related genes (Shkirkova et al., 2022; Cole et al., 2016; Manzetti and Andersen, 2016), neuroinflammation and microglia activation (Shkirkova et al., 2022; Ha et al., 2022; Cole et al., 2016; Durga et al., 2015; Gerlofs-Nijland et al., 2010; Levesque et al., 2011; Lucchini et al., 2012) as well as hall marks of neurodegeneration, e.g., neuronal death and accumulation of misfolded proteins (Shkirkova et al., 2022; Ha et al., 2022; Hullmann et al., 2017; Levesque et al., 2011). Additional *in vitro* findings support that diesel PM causes microglia activation, the release of pro-inflammatory cytokines, oxidative stress, and disruption of the blood–brain barrier integrity (Aquino et al., 2023; Levesque et al., 2013; Li et al., 2018; Roqué et al., 2016).

While the above summarized studies evaluated various endpoints indicative for and associated with neurotoxicity and neurodegeneration, the impact of (bio)diesel engine combustion-derived PM2.5 (PMDEP; PMBIO) on neuronal function has not been studied previously. Moreover, based on *in vivo* findings, we hypothesized that PM-induced effects in the lung (e.g., inflammation) can exert secondary effects on neuronal health and function. This is the first study using a novel integrated *in vitro* approach to study the indirect (systemic) effects of particles on brain function. A comparable approach was previously used to study the neuromodulatory and neurotoxic effects of tobacco smoke and e-cigarette vapor (Staal et al., 2022). We here report for the first time the effects and potency of PMDEP and PMBIO on neuronal function upon direct exposure of neuronal cultures, which is relevant considering the ability of particles to access the brain directly via the olfactory route. Furthermore, we compare the effects following direct exposure to indirect (inhalation) exposure as well as the neurotoxic potency of PMDEP vs. PMBIO.

More specifically, we first investigated the effects of exposure to diesel fuel combustion-derived PM (PMDEP), biodiesel fuel combustion-derived PM (PMBIO) and clean carbon particles (CP) (surrogate for the core of combustion-derived PM) in an *in vitro* lung model. Next, we used the medium from the basal compartment of the lung model to expose an *in vitro* brain model to assess indirect neurotoxic effects. Finally, we investigated the direct effects of PMDEP, PMBIO and CP, as well as pro-inflammatory stimuli on neuronal function using microelectrode array (MEA) recordings and cell viability measurements for comparison of direct brain exposure with simulated inhalation exposure (Fig. 1).

2. Material and methods

2.1. Chemicals

Neurobasal-A (NBA) medium, L-glutamine (200 mM), Penicillin/Streptomycin (5.000 U/mL), Penicillin/Streptomycin (10.000 U/mL), B-27 Plus supplement (50X), minimum essential medium + GlutaMAX (MEM), Fetal Bovine Serum (FBS), GlutaMAX-I (100x), Non-essential amino acid (NEAA) solution (100x), RPMI-1640 medium, MEM without phenol red, 0.05 % trypsin-EDTA, and Accutase were obtained from Life Technologies (Bleiswijk, The Netherlands). All other chemicals, unless otherwise noted, were purchased from Sigma–Aldrich (Zwijndrecht, The Netherlands).

2.2. Generation and sampling of PM test material

EN590 compliant diesel (Diesel; containing 7 % biofuel) and EN590 diesel supplemented with 50 % rapeseed methyl-ester (compliant with EN14214; Biodiesel) were used to generate the PM samples for this study. Diesel and Biodiesel fuel-derived emission were generated using a 100 kVA common rail diesel generator, which was strained using heaters. Part of the exhaust was drawn into a High Volume Cascade Impactor sampler (Cassee et al., 2003), which selects and samples the different PM size fractions. PM2.5 fraction was collected on polyurethane substrate filters (Butraco, WEMA Machinenschutz Elemente, Germany).

Carbon particles (CP) with an average primary size of 60 nm (measured using differential mobility analysis; data not shown) were generated via spark ablation (1.3 kV, 8.0 mA, 5 L/min N2) using a VSP-G1 Nanoparticle Generator (VSParticle, Delft, the Netherlands) equipped with carbon electrodes as source material and collected on fluoropore membrane filters (3 μm pore size; Merck Millipore, Darmstadt, Germany). Polyurethane substrate filters and fluoropore membrane filters were washed with methanol and dried before weighting and subsequent use for particle sampling.

2.3. Filter extraction for in vitro testing

Polyurethane substrate and fluoropore membrane filters were weighted to determine sampled particle mass. Diesel and Biodiesel fuel-derived PM (PMDEP and PMBIO), and CP were extracted from the filters using methanol as described previously (Gerlofs-Nijland et al., 2013). After extraction, samples were dried overnight at 25 °C under constant nitrogen flow to prevent oxidation of the particles.

For exposure of the lung model via nebulization, PMDEP, PMBIO, and CP were dispersed on the day of exposure in 100 % DMSO to a stock of 100 mg/mL and vortexed at full speed for 1 min. Next, particle stocks were diluted in saline solution (0.009 % NaCl in sterile ddH_2O) to 1 mg/mL containing 1 % DMSO, sonicated (20 min; ultra-sonic bath), and used

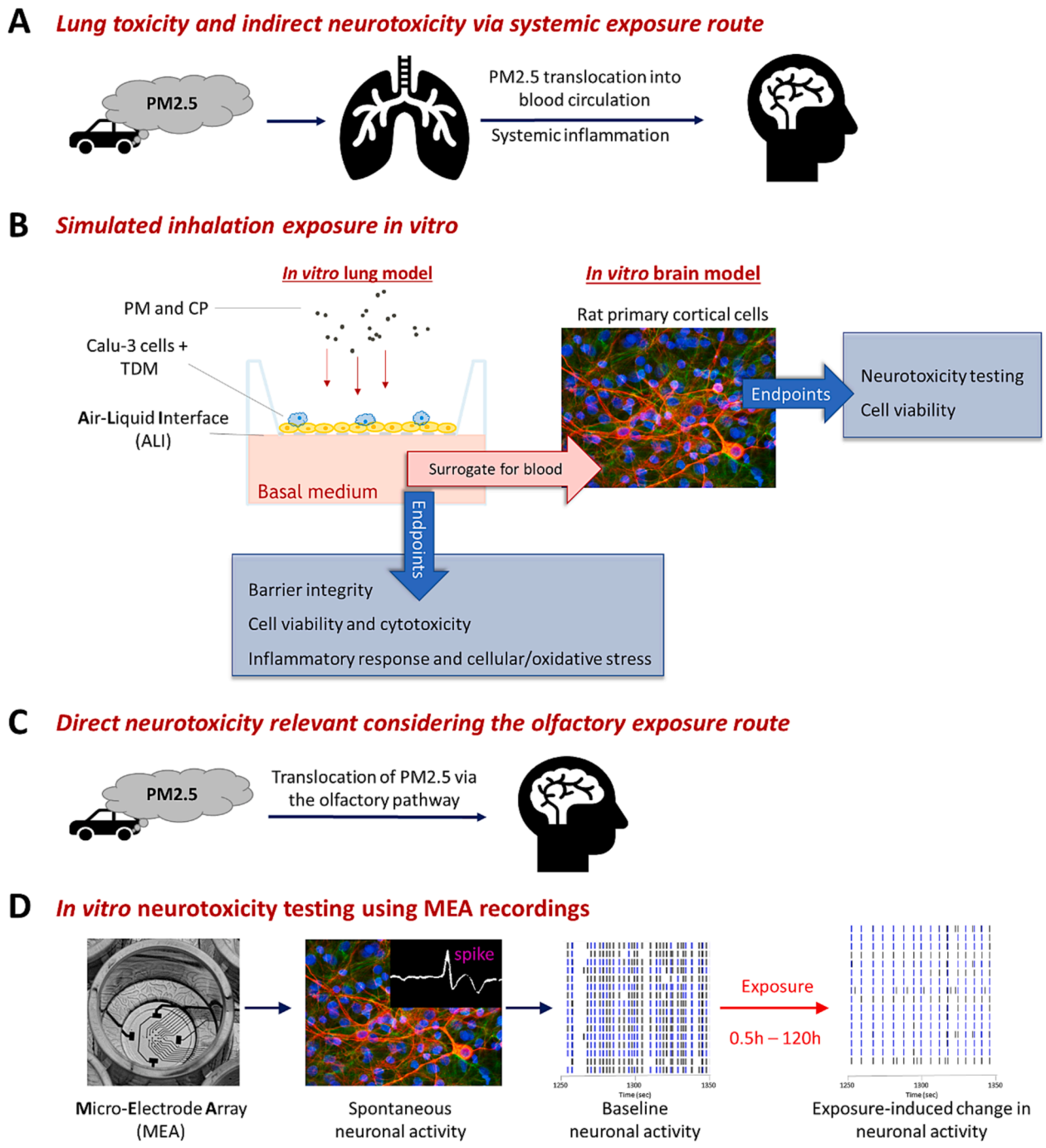

Fig. 1. Schematic overview of the study design. **A)** PM2.5 can reach the lung upon inhalation, where it can induce local inflammation and toxicity. PM2.5 may not only affect the lung, but it may reach the brain via translocating to the systemic circulation after inhalation. Moreover, PM2.5-induced inflammatory factors may impact neuronal health. **B)** Indirect effect of diesel PM2.5 (PMDEP) and biodiesel PM2.5 (PMBIO) following inhalation exposure were studied by first exposing an *in vitro* lung model via PM2.5 nebulization and secondly, after 48 h exposure, collecting basal medium to expose the *in vitro* brain model and finally performing neurotoxicity screening as depicted in **D**. Further, PM2.5-induced effects on the lung model were studied by assessing barrier function, cell viability and cytotoxicity, inflammation, and cellular and oxidative stress. **C)** PM2.5 generated by the combustion of diesel or biodiesel fuel can also enter the brain translocation via the olfactory pathway, highlighting the relevance of assessing direct neurotoxic effects *in vitro*. **D)** Direct effects of PMDEP and PMBIO on spontaneous neuronal (network) activity were assessed using microelectrode array (MEA) recordings, which are commonly used for neurotoxicity screening.

for nebulization or measurements of size distribution (see supplementary data; Table S1 and Fig. S1).

For direct exposure of primary cortical culture, PMDEP, PMBIO, and CP were first dispersed in 100 % DMSO to a stock of 100 mg/mL, vortexed at full speed for 1 min, and used directly or stored at −20℃ for further experiments (only PMDEP and PMBIO). Just prior to exposure, particle stocks were diluted to 1 mg/mL with glutamate-free culture medium (500 mL Neurobasal-A supplemented with 14 g sucrose, 1.25 mL L-glutamine (200 mM), 5 mL penicillin/streptomycin (5.000 U/mL) and 10 mL B–27 Plus Supplement (50X); pH 7.4). After sonication (20 min; ultra-sonic bath), particle stocks were further diluted with glutamate-free culture medium to a dose range of 10–1.000 µg/mL containing 1 % DMSO.

2.4. In vitro lung model and ALI exposure

2.4.1. Cell culture

The *in vitro* lung model consist of Calu-3 cells and THP-1-derived macrophages (TDMs) cultured at the air–liquid interface (ALI). Calu-3 cells (ATCC, Rockville, MD, USA; passage 10–16) were cultured in MEM medium (MEM supplemented with 10 % FBS, 1 % NEAA solution and 1 % penicillin/streptomycin (10.000 U/mL)) and THP-1 monocyte-like cell line (ATCC, Rockville, MD, USA; passage 8–13) were cultured in RPMI medium (RPMI-1640 medium with 10 % FBS and 1 % penicillin/streptomycin (10.000 U/mL)) at 95 % humidity, 37 °C and 5 % CO_2.

2.4.2. Creating the in vitro lung model

Calu-3 cells were seeded (1.2×10^5) on the apical side of transwell inserts (0.4 μm pore, 1.12 cm^2 polyester membrane, Corning Inc., Germany) in 0.5 mL MEM media. At the basal side, 1 mL MEM medium was added and cells were cultured for 12–13 days under submerged conditions at 95 % humidity, 37 °C and 5 % CO_2 before cells were moved to ALI by removing apical media.

After 5 days culture at the ALI (2 days before exposure), basal medium was replaced by MEM medium with low FBS content (MEM supplemented with 1 % FBS, 1 % NEAA solution and 1 % penicillin/streptomycin (10.000 U/mL)). Further, THP-1 monocyte-like cells were differentiated into THP-1-derived macrophages (TDMs) by addition of phorbol 12-myristate 13-acetate (PMA, 50 nM) for 24 h. The next day (one day before exposure), Calu-3 cells were co-cultured with TDMs. To do so, differentiated TDMs were gently detached using Accutase, resuspended in MEM medium, and TDMs (5×10^4) were seeded on top of Calu-3 monolayer and allowed to attach overnight.

2.4.3. Transepithelial electrical resistance measurements

The transepithelial electrical resistance (TEER), an important indicator for the barrier function of the Calu-3 monolayer, was measured in triplicates using an Evom2 Volt-Ohmmeter with 4 mm chopstick electrodes (World Precision Instruments Inc., FL, USA) as described previously (Braakhuis et al., 2020). Values were corrected for the resistance of cell-free inserts (≈130 Ω) and insert surface area (1.12 cm^2). TEER measurements were performed for all inserts before exposure and served as quality criteria to exclude inserts with insufficient barrier integrity (<800 Ω/cm^2) from experiments. After 48 h exposure, TEER was measured for three inserts (*n*) per exposure conditions and reported values represents the average TEER ratios ($TEER_{after\ exposure}/TEER_{before\ exposure}$) of 2 independent experiments (*N*). Values > 2x standard deviation (SD) above or below average are considered to be outliers and excluded from the analysis (0 % outliers in ALI control inserts; 1.9 % outliers in exposed inserts).

2.4.4. Particle exposure of the in vitro lung model

On the day of exposure, TEER was measured (for details see section 2.4.3), apical medium (which was added for the TEER measurement) was removed again and the co-culture was exposed to the particles suspended in saline solution (1 mg/mL). All inserts were exposed to three subsequent nebulization steps of 200 μL using a modified VITROCELL® cloud exposure system (Vitrocell, Waldkirch, Germany; for detail see He et al., 2020). The modified system uses a cylindric exposure chamber instead of a cuboidal unit to reduce the possibility of unequal particle deposition. Each exposure, including the three nebulization steps, took in total 30 min. In order to archive different dose levels, cells were exposed by nebulizing one (low dose), two (medium dose) or three (high dose) times 200 μL of the particle suspension (see Table 1). For the remaining nebulization steps, inserts were exposed using the control saline solution (2x for low dose, and 1x for medium dose). The average particle mass deposited during exposure amounted to 1.2, 2.1 and 3.9 μg/cm^2 for the low, medium and high dose exposure (Table 1). Control inserts were exposed three times to 200 μL saline solution (ALI control). Some additional inserts were exposed to lipopolysaccharide (LPS; 200 μL of 175 μg/mL; Sigma Aldrich, Zwijndrecht, The Netherlands) and served as positive control for inflammation. Directly after exposure, inserts were transferred to a plate containing 1 mL glutamate-free culture media (neuronal medium) per well and incubated for 48 h at ALI at 95 % humidity, 37 °C and 5 % CO_2.

Table 1
Exposure scheme of the *in vitro* lung model to particles via nebulization and the total deposited mass. Each group was exposed 3 times via nebulization. To achieve different doses, the *in vitro* lung model was exposed 1–3 times to the particle suspension. In order to keep the amount of nebulization steps equal between different groups, exposure to saline solution (vehicle; 0.009 % NaCl) was used to compensate for the remaining nebulization steps. Total deposited mass of particle is listed in mean ± SD [μg/cm^2].

	Control	Low	Medium	High
1. Nebulization	Saline	PM	PM	PM
2. Nebulization	Saline	Saline	PM	PM
3. Nebulization	Saline	Saline	Saline	PM
# Saline exposures	3x	2x	1x	0
# Particle exposures	0	1x	2x	3x
Deposited mass [μg/cm^2]	/	1.2 ± 0.3	2.1 ± 0.7	3.9 ± 0.7

2.4.5. Fluorescein translocation assay

Paracellular transport of Fluorescein was assessed as a second readout for barrier function after 48 h exposure to particles. Following 48 h incubation, inserts were transferred to a 12-well plate containing 1 mL Phenol red-free MEM per well, and 500 μL of 10 μM Fluorescein (in Phenol red-free MEM) was added to apical side of each insert. After 30 min, 1 h, and 2 h, 100 μL media of basal compartment (in triplicates) was transferred to transparent 96-well plate. To compensate for volume reduction in the basal compartment after 30 min and 1 h, 300 μL fresh Phenol red-free MEM was added to basal compartment. One insert was used as positive control after cell lysis (1 % Triton–X for 10 min) to determine the maximum translocation of Fluorescein per time point. Fluorescein translocation was measured at 498/520 nm (excitation/emission) and the Fluorescein concentration was determined by applying a standard curve. Per condition and experiment, fluorescein transport was assessed in three inserts (*n*) and averages of 2 independent experiments (*N*) are reported. Values > 2xSD above or below average are considered to be outliers and excluded from the analysis (0 % outliers in ALI control inserts; 4.9 % outliers in exposed inserts; 0 % outliers in positive control inserts).

2.4.6. Cell viability assay

Mitochondrial activity of the *in vitro* lung model was measured after 48 h particle exposure using an Alamar Blue assay to assess cell viability. Briefly, Alamar Blue solution (25 μM resazurin in Hanks' Balanced Salt solution) was added to apical side and incubated for 1.5 h at 37 °C, 5 % CO_2 and 95 % air atmosphere. Then, the Alamar Blue solution was transferred from each insert to a transparent 96-well and conversion of resazurin to resorufin was measured spectrophotometrically at 540/590 nm (excitation/emission). Values of exposed inserts were normalized to controls (per experiment, set to 100 %), then combined and values > 2xSD above or below average are considered to be outliers and excluded from the analysis (0 % outliers in ALI control inserts; 3.6 % outliers in exposed inserts). Metabolic activity is presented as the average of 3–4 insert (*n*) from 2 independent experiments (*N*).

2.4.7. Cytotoxicity assay

Cytotoxicity in the *in vitro* lung model was measured after 48 h particle exposure using the lactate dehydrogenase (LDH) assay (Roche Diagnostics GmbH, Mannheim, Germany) as previously described (He et al., 2020). LDH release was assessed in the apical and basal medium and values of control and exposed inserts were compared with the maximum LDH release of the positive control (lysis, set to 100 %). Reported values are averages of 5–6 inserts per condition (*n*) from 2

independent experiments (*N*). Values > 2xSD above or below average are considered to be outliers and excluded from the analysis (0 % outliers in ALI control inserts; 1.9 % outliers in exposed inserts).

2.4.8. Cytokine release

The inflammatory response of the lung epithelial cells and activation of TDMs as a result of the exposure to particles was studied by assessing the release of pro-inflammatory cytokines (IL-6, IL-8, IL-1β, TNF-α, and IP-10). Apical and basal medium samples were collected from the *in vitro* lung model after 48 h exposure, centrifuged at 150 x g for 10 min at 4 °C and supernatant was stored at –80 °C until cytokine analysis. Cytokine levels were determined in the collected samples by enzyme-linked immunosorbent assay (ELISA; DuoSet ELISA kits from R&D Systems, San Diego, CA, USA) according to manufacturer's protocols. Samples were diluted if necessary (apical: 1:1 (IL-1β and TNF-α), 1:10 (IP-10), or 1:100 (IL-6 and IL-8); basal: 1:1 (IL-6, IL-1β, TNF-α, and IP-10) or 1:10 (IL-8)). Medium collected from cells exposed to LPS served as positive control. Per condition and experiment, cytokine concentrations were assessed in samples from three inserts (*n*) and average values from 2 independent experiments (*N*) are reported. Values > 2xSD above or below average are considered to be outliers and excluded from the analysis (0 % outliers in ALI control inserts; 0 % outliers in exposed inserts).

2.4.9. Gene expression analysis

Induction of oxidative stress or cell stress response by particle exposure was assessed by gene expression analysis in two independent experiments. Total RNA was isolated from two inserts per exposure condition and experiment using the NucleoSpin™ RNA purification kit (Macherey-Nagel GmbH & Co. KG, Düren, Germany) according to the manufactures protocol. Concentration and purity of the RNA was determined using a NanoDrop 2000 spectrophotometer (Thermo Fisher Scientific, Wilmington, DE, USA). Reverse transcription was performed using the iScript™ cDNA synthesis kit (Bio-Rad, Hercules, CA, USA) according to the manufactures protocol. Then, expression of genes associated with oxidative stress response and cell stress was assessed by quantitative real-time polymerase chain reaction (qPCR) using iTaq universal SYBR® green supermix (Bio-Rad, Hercules, CA, USA) according to the manufactures protocol. Genes included in the analysis, primer sequences, and loaded cDNA amount are listed in Table S2. Each sample was tested in triplicate and a clean water control (SYBR® green supermix, primer pair and water) and reverse transcription control (SYBR® green supermix, primer pair and cDNA generated without RNA) were added to each plate. qPCRs were performed using a C1000 Thermal Cycler (Bio-Rad, Hercules, CA, USA) equipped with CFX96 Real-Time PCR Detection System (Bio-Rad, Hercules, CA, USA) and CFX Maestro software (v2.0; Bio-Rad, Hercules, CA, USA). Three reference genes (*β-actin*, *GAPDH*, and *YWHAZ*) were included and their stability across the test samples was validated using CFX Maestro software (v2.0; Bio-Rad, Hercules, CA, USA). Gene expression of each sample (insert) was determined by normalizing the Cq mean of the target gene to the Cq mean obtained for the three reference genes of the same sample using the ΔΔCq method in the CFX Maestro software v2.0. To obtain fold change values, expression of each gene was then further normalized to the mean expression of the controls from the corresponding experiment. Afterwards, data from the 2 independent experiments (*N*), in total 4 inserts (*n*) per exposure condition, were combined and averages of fold change for each gene and per condition were calculated. Values > 2xSD above or below average are considered to be outliers and excluded from the analysis (0 % outliers in ALI control inserts; 0 % outliers in exposed inserts).

2.5. In vitro brain model and neurotoxicity screening using MEAs recordings

2.5.1. Rat primary cortical cultures

Primary cortical cultures were isolated from Wistar rat pups (Envigo, Horst, the Netherlands) on postnatal day 0 to 1 (PND0-1) and cultured on Polyethyleneimine (0.1 %)-coated 48-well MEAs plates (Axion BioSystems Inc, Atlanta, USA) as described previously (Gerber et al., 2021). Animal experiments were performed in agreement with Dutch law, the European Community directives regulating animal research (2010/63/EU) and approved by the Ethical Committee for Animal Experiments of Utrecht University. All efforts were made to minimize the number of animals used and their suffering.

2.5.2. Microelectrode array (MEA) recordings

Each well of a 48-well MEA plate contains 16 nanotextured microelectrodes (40–50 μm diameter; 350 μm centre-to-centre spacing) forming an array on the culture surface that enables the detection of extracellular local field potentials (spikes) at different locations within the culture. Neuronal activity was recorded using a Maestro (direct exposure experiments) or Maestro Pro (indirect exposure experiments) 768-channel amplifier with integrated heating system, temperature controller, CO_2 controller (only for Maestro Pro) and data acquisition interface (Axion BioSystems Inc, Atlanta, USA; for direct exposure experiments). MEA recordings were performed on DIV9-14 as previously described in detail (Gerber et al., 2021).

Briefly, on DIV9, when rat primary cortical cells exhibit stable spontaneous neuronal activity (Dingemans et al., 2016; Gerber et al., 2021), a 30 min baseline recording was performed. Next, cells were exposed under sterile conditions (for details see below) and neuronal activity was measured immediately after the exposure for 0.5 h and again after 24 h (DIV10), 48 h (DIV11) and 120 h (DIV14; only for selected direct exposure experiments) continuous exposure to cover both acute and prolonged exposure scenarios. Between recordings, cortical cells were kept at 95 % humidity, 37 °C and 5 % CO_2.

For simulated inhalation exposure experiments, 125 μL (25 % of the medium in one well) of the medium was removed 1 h before the baseline recording. After the baseline recording, cells were exposed by adding 125 μL of collected ALI medium (resulting in 1:4 dilution of the ALI medium). ALI control medium (1:4 dilution) was used as control.

For direct exposure experiments, cells were exposed to 1–100 μg/mL PMDEP, PMBIO or CP, and DMSO (0.1 % final concentration) was used as control. For specific experiments testing neuromodulation by inflammatory stimuli, cells were exposed to 0.3–3000 ng/mL LPS or 0.01–100 ng/mL recombinant rat CINC-1 and TNF-α (R&D Systems, San Diego, CA, USA), and Phosphate-buffered saline (0.1 % final concentration) was used as control.

All conditions were tested on neuronal cultures originating from at least 2 different isolations, in at least 2 plates (*N*) and at least 16 wells (*n*). Axion's Integrated Studio (AxIS 1.7.8 and AxIS 3.2) was used to manage data acquisition and further data processing and analysis was performed as previously described in detail (Gerber et al., 2021). Briefly, spikes were detected using the AxIS spike detector (Adaptive threshold crossing, Ada BandFlt v2) with a post/pre spike duration of 3.6/2.4 ms and a variable threshold spike detector set at 7xSD of the internal noise level (rms) on each individual electrode. Data analysis was performed with NeuralMetric Tool (version 2.2.4, Axion BioSystems) using the last 20 min of each recording, except for acute exposure to medium collected from the *in vitro* lung model. Here, the last 10 min of the 0.5 h recording were used because of the occurrence of transient exposure effects. Only active electrodes (MSR ≥ 6 spikes/s) in active wells (≥4 active electrodes and ≥ 1 network bursts per minute during baseline recording) were included. Bursts were extracted with the Poisson Surprise method (Legendy and Salcman, 1985) with a minimal surprise, and network bursts were determined with an adaptive threshold algorithm.

For both exposure methods, the effects of PMDEP, PMBIO, CP, LPS,

CINC-1 and TNF-α on spontaneous activity were determined by comparing the baseline activity with activity following exposure (0.5 h, 24 h, 48 h, and 120 h). Means of different neuronal activity parameters (Mean Spike Rate (MSR), Mean Burst Rate (MBR) and Mean Network Burst Rate (MNBR)) were calculated based on well averages and normalized to control as previously described (Gerber et al., 2021). Results are expressed as average in % of control and wells that showed an effect > 2xSD above or below average were considered outliers and removed from further data analysis (for direct exposure: 2.3 % outliers in control wells and 4.2 % outliers in exposed wells; for simulated inhalation exposure: 2.1 % outliers in control wells and 4.8 % outliers in exposed wells).

2.5.3. Cell viability assay

After the final MEA recordings were completed, i.e. 48 h (indirect exposure, direct LPS exposure) or 5 days (direct PM exposure) after the start of the exposure, an Alamar Blue assay was performed to measure mitochondrial activity as previously described (Gerber et al., 2021) and data were analyzed as described in 2.4.6. Wells that showed an effect > 2xSD above or below average were considered outliers and removed from further data analysis (for direct exposure: 2.7 % outliers in control wells and 6.7 % outliers in exposed wells; for indirect exposure: 2.1 % outliers in control wells and 2.8 % outliers in exposed wells).

2.6. Statistics

All statistical analyses were performed using GraphPad Prism software (v9.3.1, GraphPad Software, La Jolla CA, USA). If applicable, non-linear regressions were used to fit dose–response curves and PROAST web application (v70.1, RIVM, the Netherlands) was used to compute benchmark doses (BMD) values using the SD of controls as benchmark response level. Dose-dependent effects were determined by one-way ANOVA followed by a *post–hoc* Dunnett test comparing values obtained for exposed inserts/wells to values of respective control inserts/

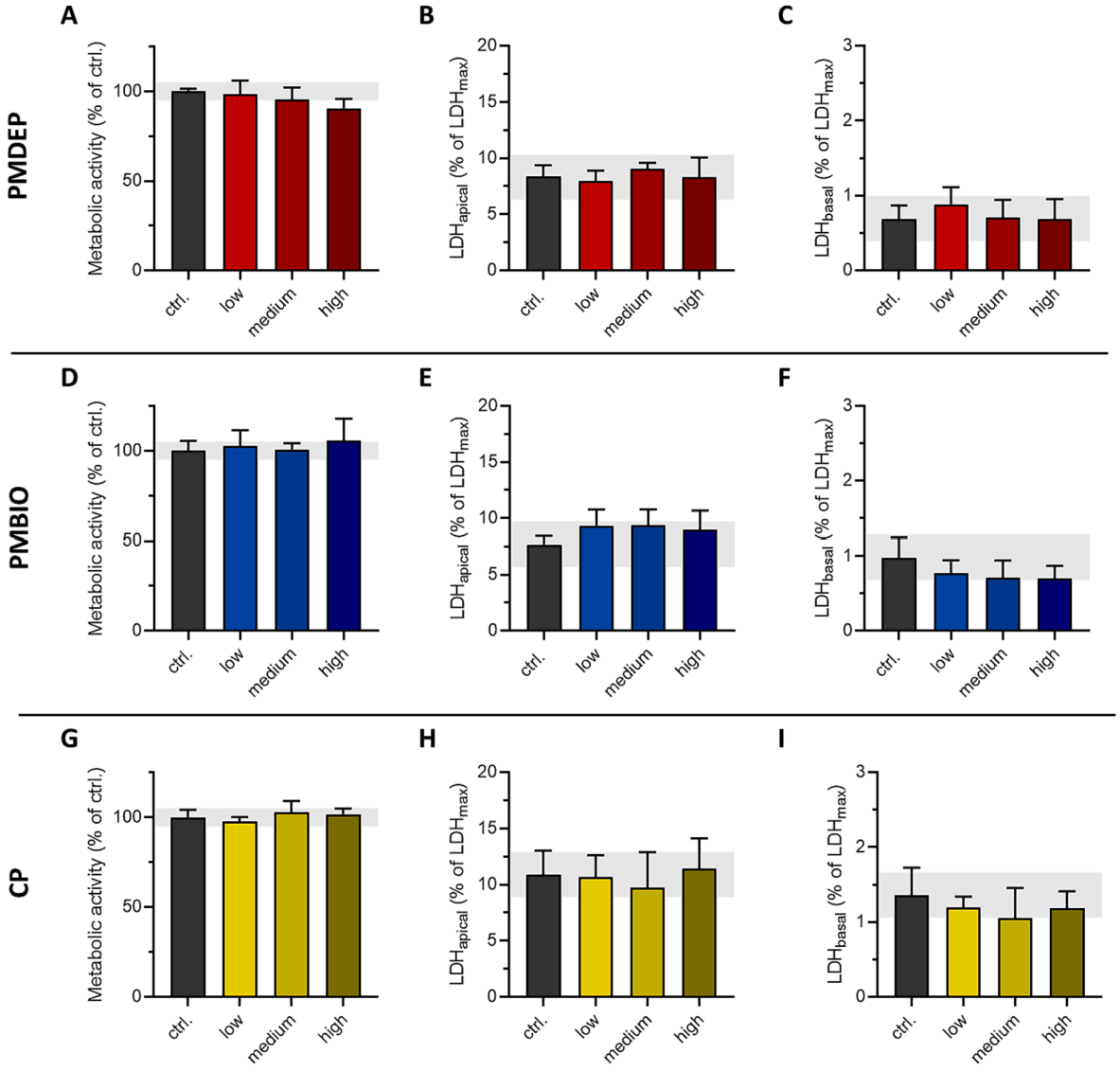

Fig. 2. Metabolic activity and LDH release in the *in vitro* lung model following 48 h exposure to PMDEP (top; red), PMBIO (middle; blue) or CP (bottom; green). Inserts were exposed to vehicle solution only (control) or to 1 (low), 2 (medium), and 3 (high) doses of particle suspension. **A), D)** and **G)** Metabolic activity is expressed as mean ± SD in % of control (control set at 100 %) from $n = 3$–6 inserts, $N = 2$ independent experiments. Grey area indicates 95–105 % metabolic activity (based on average SD of controls (±5%)), which is used as threshold for relevant effects. LDH release to apical (**B**, **E**, and **H**) and basal (**C**, **F**, and **I**) compartment expressed as mean ± SD in % of LDH_{max} (set at 100 %) from $n = 3$–6 inserts, $N = 2$ independent experiments. Grey areas indicate ± 2 % or ± 0.3 % LDH leakage (based on average SD of controls) into apical and basal compartment, respectively, which is used as threshold for relevant effects. (For interpretation of the references to colour in this figure legend, the reader is referred to the web version of this article.)

wells. Differences were considered statistically significant if p–values < 0.05. For all endpoints, differences were considered relevant when the effect was larger than the benchmark response level, i.e. 1xSD of the control. All data were derived from at least 2 independent experiments (N) and are presented as mean ± SD, except for MEA data which are traditionally presented as mean ± standard error of the mean (SEM).

3. Results

3.1. Direct toxicity in an in vitro lung model

3.1.1. Cell viability and cytotoxicity

We first investigated the effect of 48 h exposure to a low, medium, or high dose of PMDEP, PMBIO or CP (1 to 3 times exposure to particle suspension via nebulization, resulting in 1.2–3.9 μg/cm^2; see Table 1) on the *in vitro* lung model. As depicted in Fig. 2, the highest dose of PMDEP modestly but not significantly reduced metabolic activity (Fig. 2A, 91 % of control), without affecting LDH leakage in the apical (Fig. 2B) or basal (Fig. 2C) compartment, suggesting that PMDEP exposure did not cause

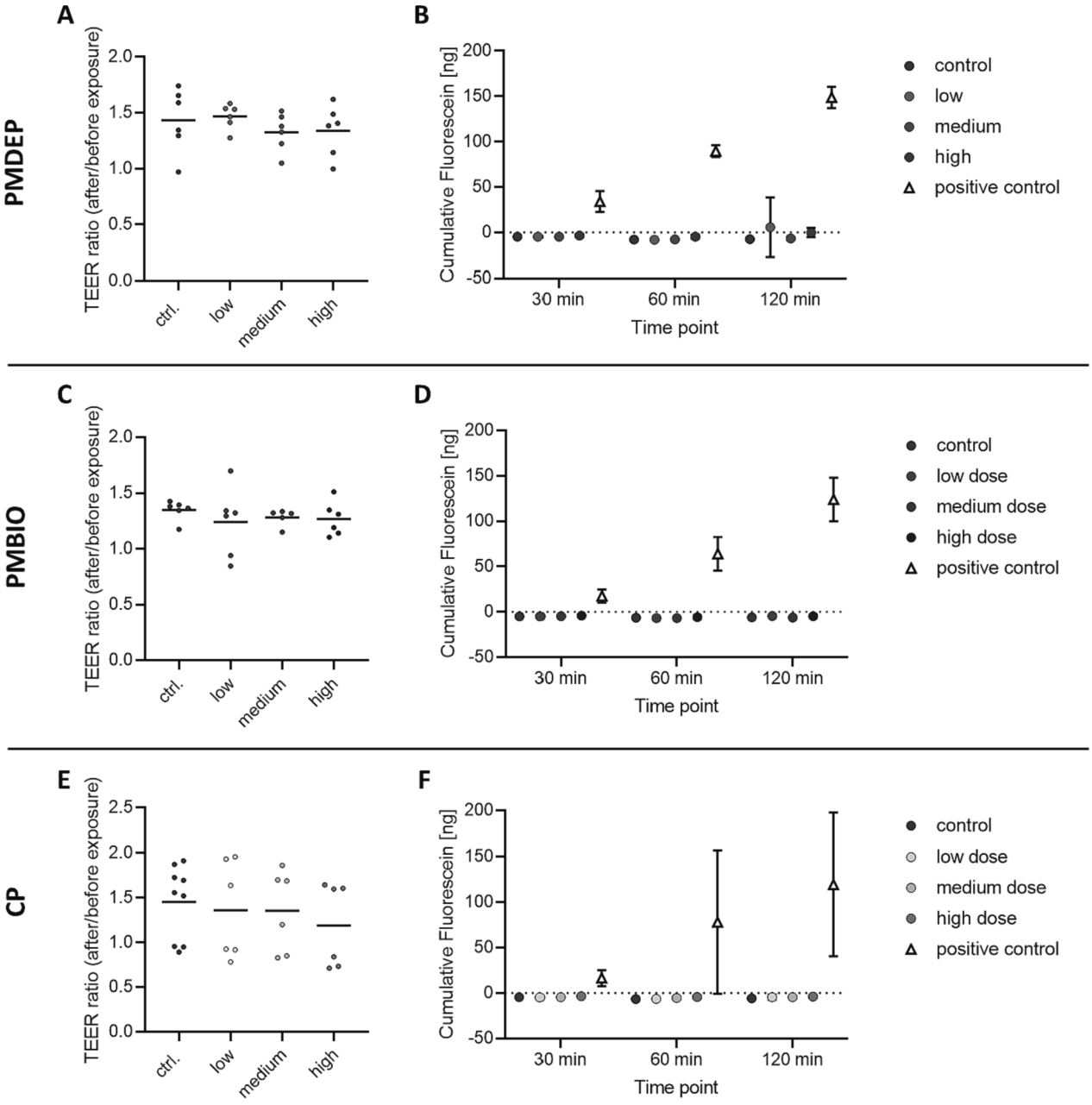

Fig. 3. Barrier function of the *in vitro* lung model following 48 h exposure to PMDEP (top; red), PMBIO (middle; blue), or CP (bottom; green). Inserts were exposed to vehicle solution only (control) or to 1 (low), 2 (medium), and 3 (high) doses of particle suspension. **A), C)** and **E)** TEER data are presented as ratio of resistance (Ω/cm^2) measured after 48 h exposure to values measured before exposure. The solid lines indicate the mean obtained from the individual inserts represented by the dots (n = 6–9 inserts, N = 2 independent experiments). **B), D)** and **F)** Fluorescein translocation is presented as cumulative Fluorescein (mean ± SD in ng) detected in the basal compartment after 30 min, 60 min, and 120 min from n = 5–6 inserts, N = 2 independent experiments. Additionally, cumulative Fluorescein translocation of lysed inserts (positive control; n = 3, N = 2) is depicted. Dotted line indicates zero line, i.e., no Fluorescein translocation. (For interpretation of the references to colour in this figure legend, the reader is referred to the web version of this article.)

overt cytotoxicity. For PMBIO and CP, neither metabolic activity (Fig. 2D and 2G) nor LDH release (Fig. 2E–F and 2H–I) were affected indicating that these exposures also did not induce cytotoxicity in the *in vitro* lung model.

3.1.2. Barrier function

Next, we studied the impact of exposure to PMDEP, PMBIO or CP on the barrier function of the *in vitro* lung model by assessing TEER and performing an Fluorescein translocation assay. Following 48 h exposure, the TEER ratio (value after exposure vs. value before exposure) of inserts exposed to PMDEP, PMBIO or CP did not differ from the ratio obtained for control inserts (Fig. 3A, 3C, and 3E). Similarly, no relevant increase in Fluorescein translocation was detected in basal medium of PMDEP-, PMBIO- or CP-exposed inserts indicating that barrier function was not affected by the exposures (Fig. 3B, 3D, and 3F). In contrast, for inserts with lysed cells (positive control) clear time-dependent translocation of Fluorescein into the basal compartment was measured.

3.1.3. Inflammatory response

Following 48 h exposure to PMDEP, PMBIO, or CP, the inflammatory response of the *in vitro* lung model was assessed by measuring the cytokine concentration in the apical and the basal medium. Concentrations in apical and basal medium from control inserts of the CP exposure experiments (ctrl.$_{CP}$) were substantially lower than concentration from control inserts of the experiments studying PM (ctrl.PM; see Fig. 4, Table S3 and S4). Data from the different controls are therefore not merged and results for particle- and LPS-exposed insets are compared to their respective controls. For LPS, exposure was either performed together with PMDEP and PMBIO exposure (red/blue circle) or with CP exposure (green circle).

Concentrations of IL-8, IL-6, IP-10, and IL-1β in apical medium obtained from PMDEP- and PMBIO-exposed inserts did not differ from ctrl. PM, although LPS exposure induced a 3- to 10-fold increase in the cytokine concentrations (Fig. 4, Table S3). Similarly, in CP-exposed inserts, apical medium concentration of IL-8, IL-6, IP-10, and IL-1β did not differ from concentration measured in medium from control inserts (ctrl.$_{CP}$), although LPS exposure caused an 4.5- to 11-fold increase of these cytokines (Fig. 4, Table S4). TNF-α was detected only in the apical medium collected from the LPS-exposed inserts, whereas in none of the other apical medium samples (ctrl.PM, ctrl.$_{CP}$, PM exposure, CP exposure) TNF-α was detected at concentrations exceeding the detection limit of the ELISA kit (Fig. 4I, indicated by N.D.; Table S3 and S4).

Results for basal medium were comparable to those obtained for apical medium samples. Samples from PM- and CP-exposed inserts did not show any effects on IL-8 and IL-6 concentrations, although cytokine levels were higher (ca. 2–7.5 -fold increase) in LPS-exposed inserts (Fig. 8B and 8D, Table S3 and S4). For IP–10, IL-1β, and TNF-α, concentrations in basal medium of controls and inserts exposed to PM or CP did not exceed the detection limit (Fig. 4F, 4H and 4 J indicated by N.D.; Table S3 and S4).

Together, these data indicate that exposure to PM and CP did not induce overt inflammation of the *in vitro* lung model following 48 h of exposure, although the model is sensitive to inflammatory stimuli like LPS.

3.1.4. Oxidative and cell stress

Finally, oxidative stress or general cell stress in the *in vitro* lung model following 48 h exposure to PMDEP, PMBIO, or CP were assessed by gene expression analysis. As depicted in Fig. 5, neither PMDEP nor PMBIO caused clear dose–response related changes in any of the genes associated with oxidative stress or cell stress (also see Fig. S2 and S3 for fold change values of individual inserts after PMDEP or PMBIO exposure).

Nonetheless, low and medium dose of PMBIO (but not the high dose) increased GPX, indicative for oxidative stress. Notably, CYP1A1 was increased by exposure to the medium and high dose of PMDEP, or all three dose levels of PMBIO, even though the increase was only significant for the medium dose of PMDEP and PMBIO. In contrast to PM exposure, none of the CP exposures affected CYP1A1 expression, suggesting that adsorbed chemicals on the carbon core surface of PMDEP and PMBIO, e.g., PAH, cause the overexpression of CYP1A1. Overall, fold change of gene expression following CP exposure were less pronounced compared to PM samples (also see Fig. S4 for fold change values of individual inserts after CP exposure). Nevertheless, following high dose exposure, HO1 and p53 were significantly increased indicative for (modest) oxidative stress and cell/DNA damage.

3.2. Neurotoxicity assessment in the in vitro brain model following simulated inhalation exposure to PMDEP, PMBIO, and CP

Since the above exposure conditions did not induce overt or non-specific toxicity to the *in vitro* lung model, we investigated in a next step the impact of the lung exposure to PM and CP on the brain. We used the basal medium collected from the *in vitro* lung model previously exposed at the air–liquid interface (ALI) for 48 h to vehicle control (ALI ctrl.), PMDEP, PMBIO, or CP, to expose the *in vitro* brain model (rat primary cortical cells), and thereby mimicked neurotoxic effects of inhalation exposure *in vitro*. Changes in neuronal network activity, as a measure for neurotoxicity, can be recorded using MEAs, which provide a non-invasive, sensitive and integrated readout for several critical cellular and molecular mechanisms underlying neuronal function (Johnstone et al., 2010; McConnell et al., 2012; Valdivia et al., 2014).

Interestingly, acute exposure to medium collected from the vehicle control of the *in vitro* lung model (ALI ctrl.) somewhat reduced neuronal activity compared to exposure to neuronal medium (not used to culture the *in vitro* lung model). While MSR, MBR and MNBR were reduced on average to respectively 89 %, 71 % and 75 % of neuronal medium control the decrease in neuronal activity upon acute exposure to the ALI ctrl vs. neuronal medium control is variable between all experiments (Fig. 6A). To overcome the inter-experimental variation, MEA data upon indirect exposure has been normalized to the more stable neuronal medium control. After 24 h and 48 h exposure, however, neuronal activity of cells exposed to medium from ALI ctrl. did not differ from cells exposed to neuronal medium control. Furthermore, exposure to ALI ctrl. did also not affect metabolic activity after 48 h (Fig. 7). Therefore, effects of medium collected from the PM and CP exposed *in vitro* lung model were evaluated by comparing the neuronal activity to neuronal medium and ALI ctrl. exposure.

Overall, the most profound changes in neuronal activity, specifically increased MSR, were observed during acute exposure (Fig. 6A). Compared to neuronal medium control, acute exposure to medium from inserts exposed to PMDEP and medium and high dose of PMBIO increased MSR to 158 % and 152–153 %, respectively. The medium and high dose of PMBIO also increased the MNBR. Further, medium collected from high dose CP exposure increased MSR following acute exposure, although this effect was only significantly when compared to corresponding ALI ctrl. medium. In contrast, MBR following CP exposure modestly decreased when compared to neuronal medium control but did not differ from ALI ctrl..

Notably, MSR of rat primary cortical cells remained increased following 24 h exposure to PMBIO-exposed medium (Fig. 6B, low and high dose). Besides this increase, none of the exposure conditions caused consistent changes in the neuronal activity of the rat primary cortical cells following prolonged (24–48 h) exposure (Fig. 6B–C) and metabolic activity was unaffected (Fig. 7) suggesting that neuronal cells were not stressed by prolonged exposure to medium from *in vitro* lung model.

3.3. Direct neurotoxicity of PMDEP, PMBIO and CP in the in vitro brain model

PM can also reach the brain directly via the olfactory route, highlighting the relevance of studying direct neurotoxicity. Furthermore,

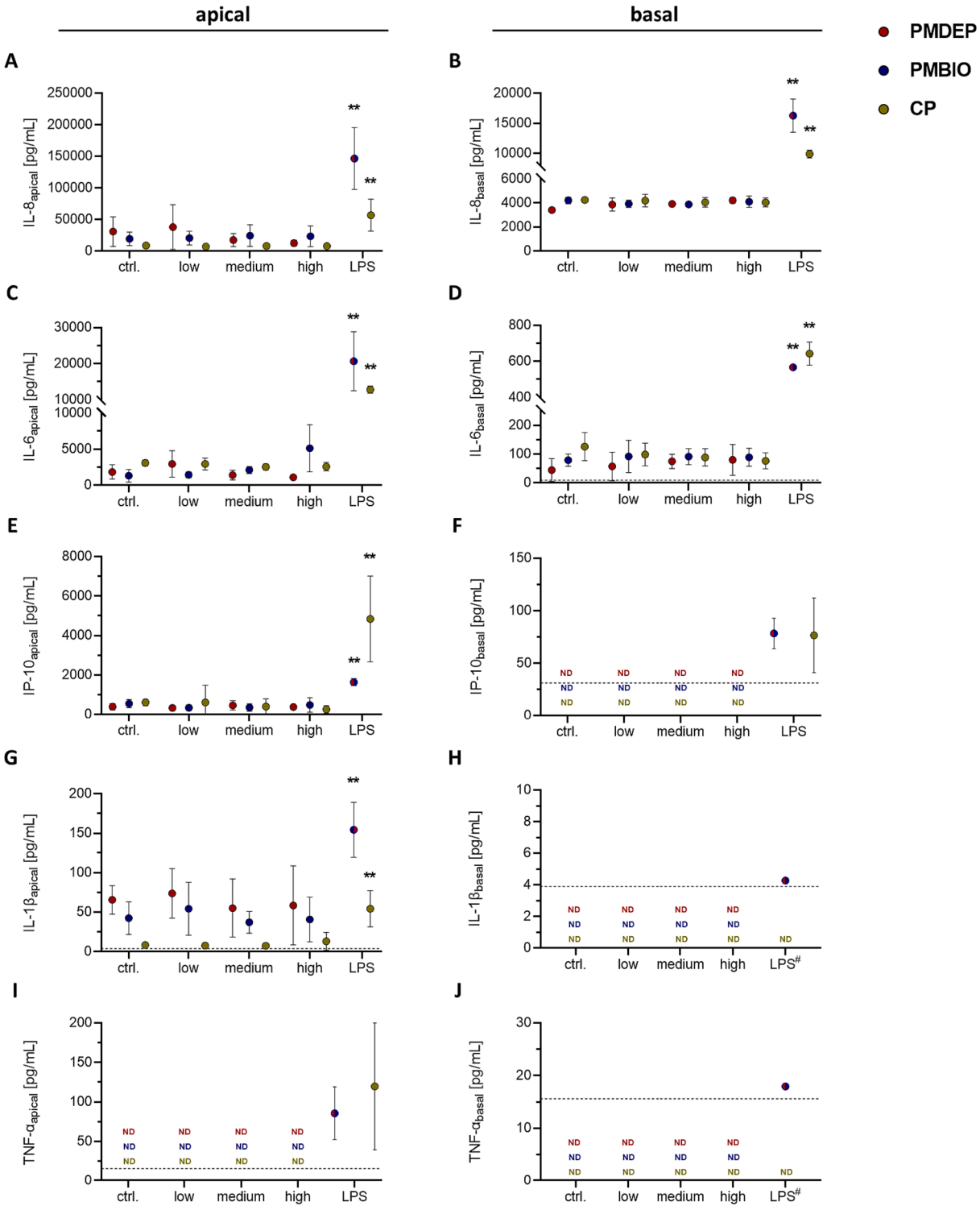

Fig. 4. Cytokine release in the *in vitro* lung model following 48 h exposure to PMDEP (red), PMBIO (blue), or CP (green). Inserts were exposed to vehicle solution only (control), LPS (positive control; red/blue circle when performed in the same experiment as PMDEP and PMBO exposure; green circle when performed in the same experiment as CP exposure), or to 1 (low), 2 (medium), and 3 (high) doses of particle suspension. Cytokine concentrations were measured in apical (left) and basal medium (right). Cytokine levels (IL-8, IL-6, IP-10, IL-1β, and TNF-α) are presented as mean ± SD from $n = 11–12$ inserts (control) or $n = 5–6$ inserts (PM or CP exposure), from $N = 2$ independent experiments. For PMBIO high dose exposure, IL-6 was derived from 3 inserts (n), 1 independent experiment (N) only. For LPS, cytokines levels (mean ± SD) were measured in medium from $n = 3$ inserts, from $N = 1$ experiment. IL-1β and TNF-α were only detected in basal medium of 1 insert exposed to LPS, highlighted by LPS$^{\#}$. Dotted line indicates the detection limit of the ELISA kits (IL-8 and IP-10: 31.3 pg/mL, TNF- α: 15.6 pg/mL, IL-6: 9.4 pg/mL, and IL-1 β: 3.9 pg/mL). N.D., not detected. ** $p < 0.01$ compared to control. (For interpretation of the references to colour in this figure legend, the reader is referred to the web version of this article.)

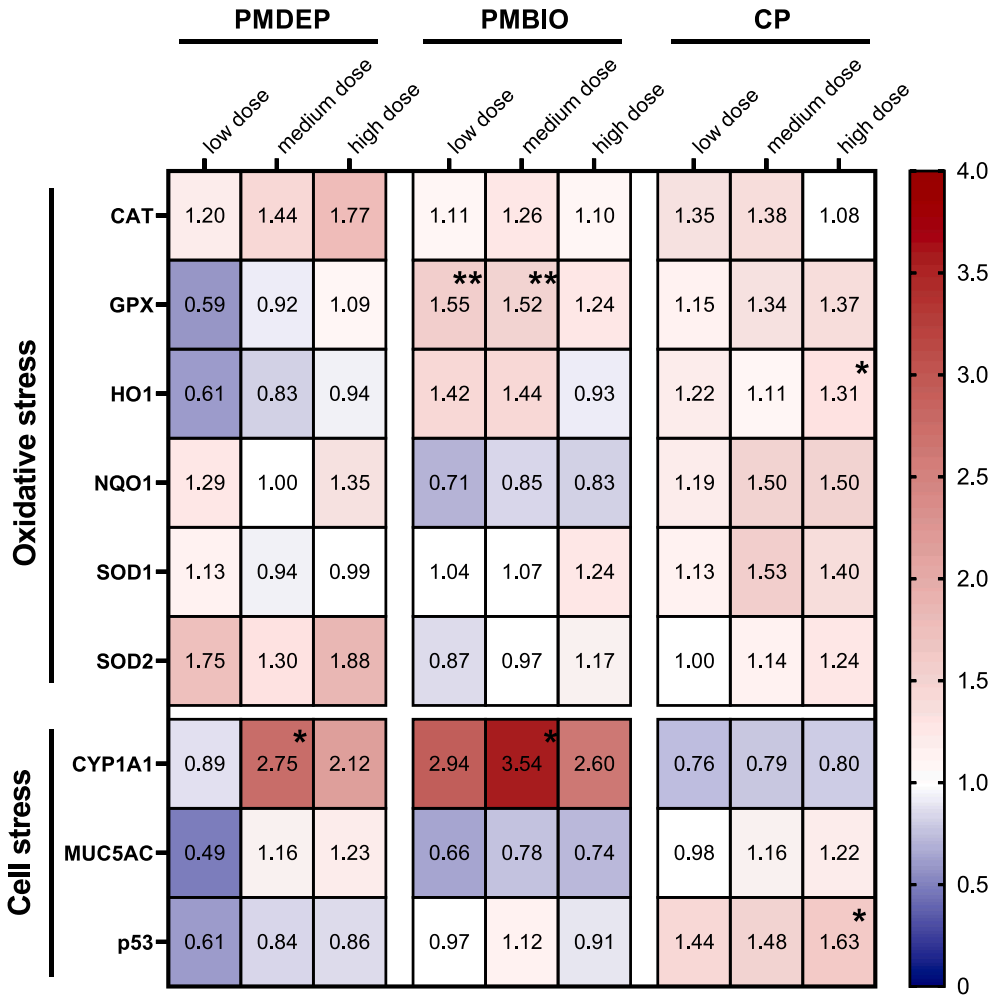

Fig. 5. Change in gene expression of the *in vitro* lung model following 48 h exposure to PMDEP, PMBIO, or CP to assess oxidative stress and cell stress. Cells depict fold change of mRNA expression associated with oxidative stress and cell stress response. Values in cells represent mean of fold change normalized to controls (=1.00) from 4 inserts ($n = 4$) of 2 independent experiments ($N = 2$). * $p < 0.05$ compared to control; ** $p < 0.01$ compared to control. CAT, catalase; GPX, glutathione peroxidase; HO1, heme oxygenase 1; NQO1, NAD(P)H quinone dehydrogenase 1; SOD1, superoxide dismutase 1; SOD2, superoxide dismutase 2; CYP1A1, Cytochrome P450 1A1; MUC5AC, mucin 5AC; p53, tumor protein p53.

direct neurotoxicity data are suitable to compare the neurotoxic potency of PMDEP, PMBIO and CP, which is important for risk assessment and evaluating the possible impact of mitigation measures. Additionally, we aimed to compare the direct neurotoxic effect with the modest and short-lived effects observed following simulated inhalation exposure. To do so, we exposed rat primary cortical cultures grown on MEAs directly to 1–100 μg particles/mL (equivalent to 1.2–119 μg/cm^2 assuming all particles will deposit on the cells) and assessed changes in neuronal activity following acute (0.5 h) and prolonged (24 h, 48 h, and 120 h) exposure.

Interestingly, none of the acute exposures affected neuronal activity, except for the high dose of PMDEP (100 μg/mL), which evoked a modest reduction of the MBR (62 % of control; Fig. 8A). On the other hand, following prolonged exposure (24 h, 48 h, and 120 h), both PMDEP and PMBIO persistently inhibited neuronal activity with comparable effect patterns in the higher dose range (≥30 μg/mL) during the 5 days of exposure (Fig. 2B–D). Interestingly, exposure to 10 μg/mL PMDEP (24 h and 48 h) already reduced neuronal activity significantly, whereas no effects are observed for 10 μg/mL PMBIO. A clear difference in the degree of inhibition is also seen following 120 h of exposure, indicating that PMDEP exhibit higher neurotoxic potency (Fig. 2B–D). The higher neurotoxic potency of PMDEP is also reflected in the computed BMD values and corresponding confidence intervals (Table 2, Fig. S5). BMD values obtained for PMDEP are 3.3–7.6 fold lower than corresponding values for PMBIO. In contrast, CP did not inhibit neuronal activity (Fig. 8B–D) following prolonged exposure indicating that clean carbon core of PM samples unlikely caused the reduction of neuronal activity.

Importantly, after 120 h exposure, no change in metabolic activity was detected in cells exposed to PMDEP and PMBIO (Fig. 9A) indicating that PM exposure did not affect cell viability. For CP exposure, fluorescence was decreased for 30 μg/mL and 100 μg/mL suggesting a decrease in cell viability (Fig. 9A). However, in a separate cell-free experiment it was shown that CP at doses > 10 μg/mL quenches the fluorescence emission of resorufin (Fig. 9B). The quenching of the signal is comparable to the presumed reduction in metabolic activity measured for exposed cells, indicating that metabolic activity actually was not affected by CP.

3.4. Neuromodulatory effect of pro-inflammatory stimuli

Since particle exposure-induced toxicity is closely linked with (neuro)inflammation, we tested if exposure to medium collected from the *in vitro* lung model previously exposed to LPS would alter spontaneous neuronal activity of the rat primary cortical culture. Furthermore, we tested the direct effects of LPS and two pro-inflammatory cytokines, CINC-1 (considered a rat equivalent to IL-8) and TNF-α, on neuronal

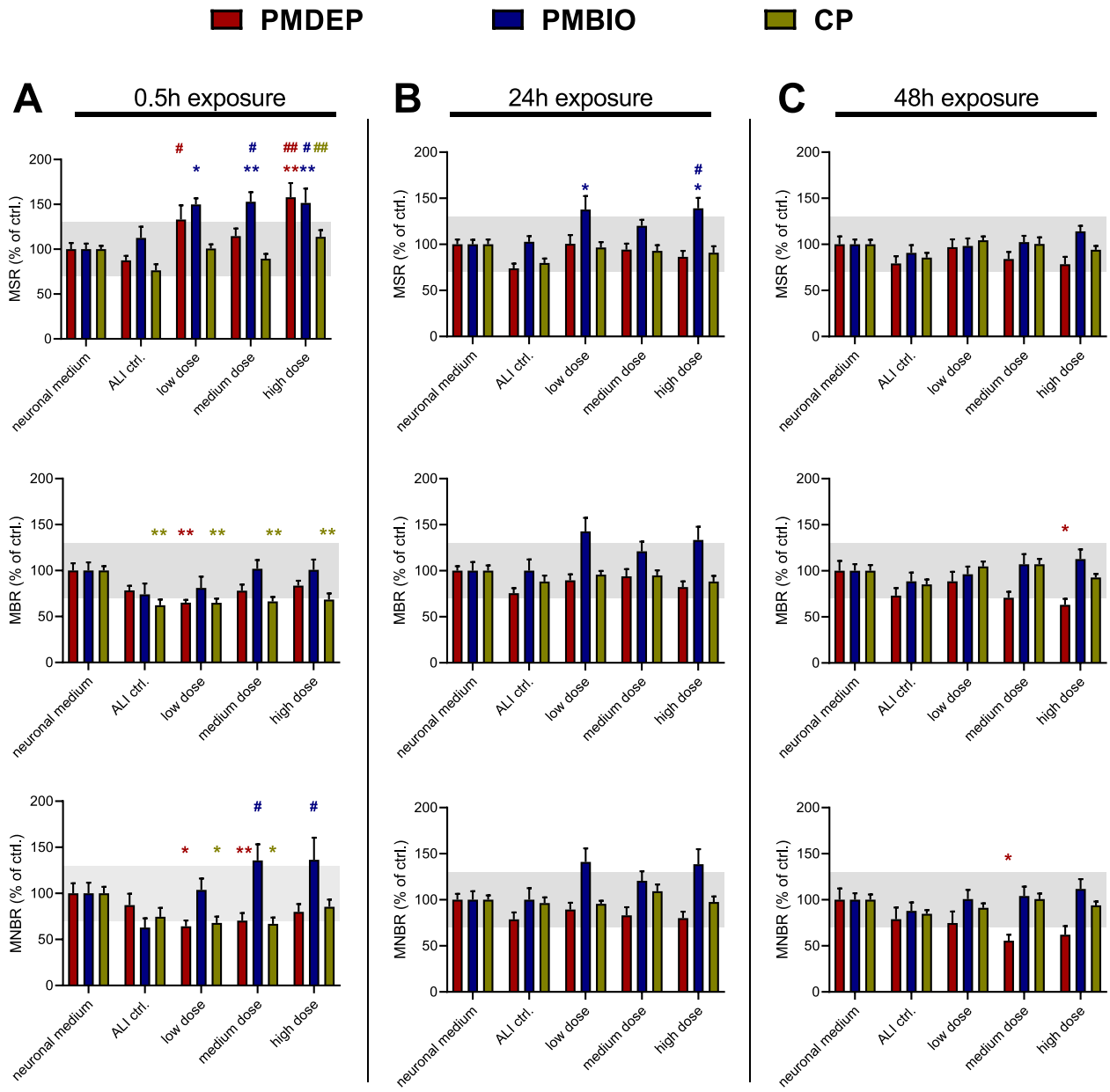

Fig. 6. Neuronal activity of rat primary cortical cells following simulated inhalation exposure to PMDEP (red), PMBIO (blue) or CP (green). Neuronal activity was recorded after 0.5 h (**A**), 24 h (**B**), and 48 h (**C**) exposure and is presented as mean spike rate (MSR; top), mean bust rate (MBR; middle), and mean network burst rate (MNBR; bottom). Data are depicted as mean treatment ratio (±SEM) in % of neuronal medium control from $n = 12–24$ wells, $N = 2–3$ plates. Grey area indicates biological variation of MEA data (based on SD of time-matched neuronal medium control), which is used as a benchmark for toxicological relevance (±30 %). * $p < 0.05$ compared to neuronal medium and exceeding the benchmark response level (grey area; ± 30 %), ** $p < 0.01$ compared to neuronal medium and exceeding the benchmark response level (grey area; ± 30 %), # $p < 0.05$ compared to ALI ctrl. medium and deviating > 30 % from ALI ctrl. medium, ## $p < 0.01$ compared to ALI ctrl. medium and deviating > 30 % from ALI ctrl. medium. (For interpretation of the references to colour in this figure legend, the reader is referred to the web version of this article.)

function.

In line with the data presented in Fig. 6, exposure to medium collected from ALI control reduced neuronal activity during acute exposure, but not following 24 h and 48 h exposure (Fig. 10). Overall, medium collected from the *in vitro* lung model previously exposed to LPS only exhibited limited effects on neuronal activity and changes are seen mainly during acute exposure (Fig. 10). The increase in MSR and MNBR attenuated following prolonged exposure and changes were no longer detected following 24 h and 48 h exposure for any of the neuronal activity parameters (Fig. 10).

Interestingly, direct acute exposure to LPS (0.3–3,000 ng/mL) did not impact neuronal activity (Fig. 11A). Following prolonged (24 h and 48 h) exposure, only MSR of cells exposed to non-cytotoxic concentration of 300 µg/mL and 3,000 µg/mL was modestly reduced (67–74 % of control), whereas no effects were observed for MBR and MNBR (Fig. 11A) indicating that LPS itself does not modulate neuronal activity. Comparable, CINC-1 did not modulate neuronal activity (Fig. 11B) and unlikely caused the excitation seen for exposure to the medium collected from the LPS-exposed *in vitro* lung model.

For TNF-α (0.01–100 ng/mL), acute exposure did not affect spontaneous neuronal activity (Fig. 11C), whereas prolonged exposure to 10 ng/mL (only MNBR at 24 h) and 100 ng/mL TNF–α resulted in modest but consistent reduction of overall neuronal activity (Fig. 11C; MSR: 64–67 % of control, MBR: 67–73 % of control, and MNBR: 59 % of

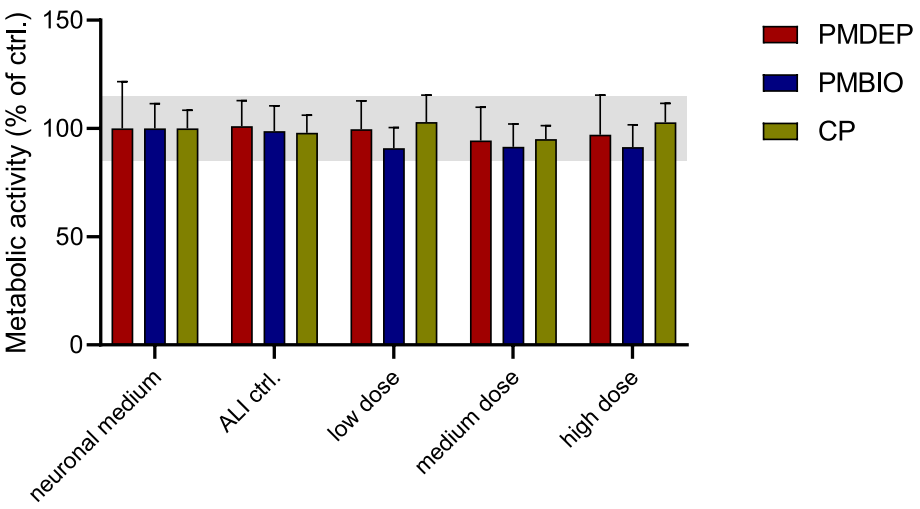

Fig. 7. Metabolic activity of the *in vitro* brain model following simulated inhalation exposure to PMDEP (red), PMBIO (blue) or CP (green). Metabolic activity of rat primary cortical cultures after 48 h exposure is depicted as mean (±SD) in % of neuronal medium control from $n = 15–26$ wells, $N = 2–3$ plates. Grey area indicates 90 %–110 % cell neuronal medium viability (SD of control), which is used as a threshold for relevant changes in cell viability. (For interpretation of the references to colour in this figure legend, the reader is referred to the web version of this article.)

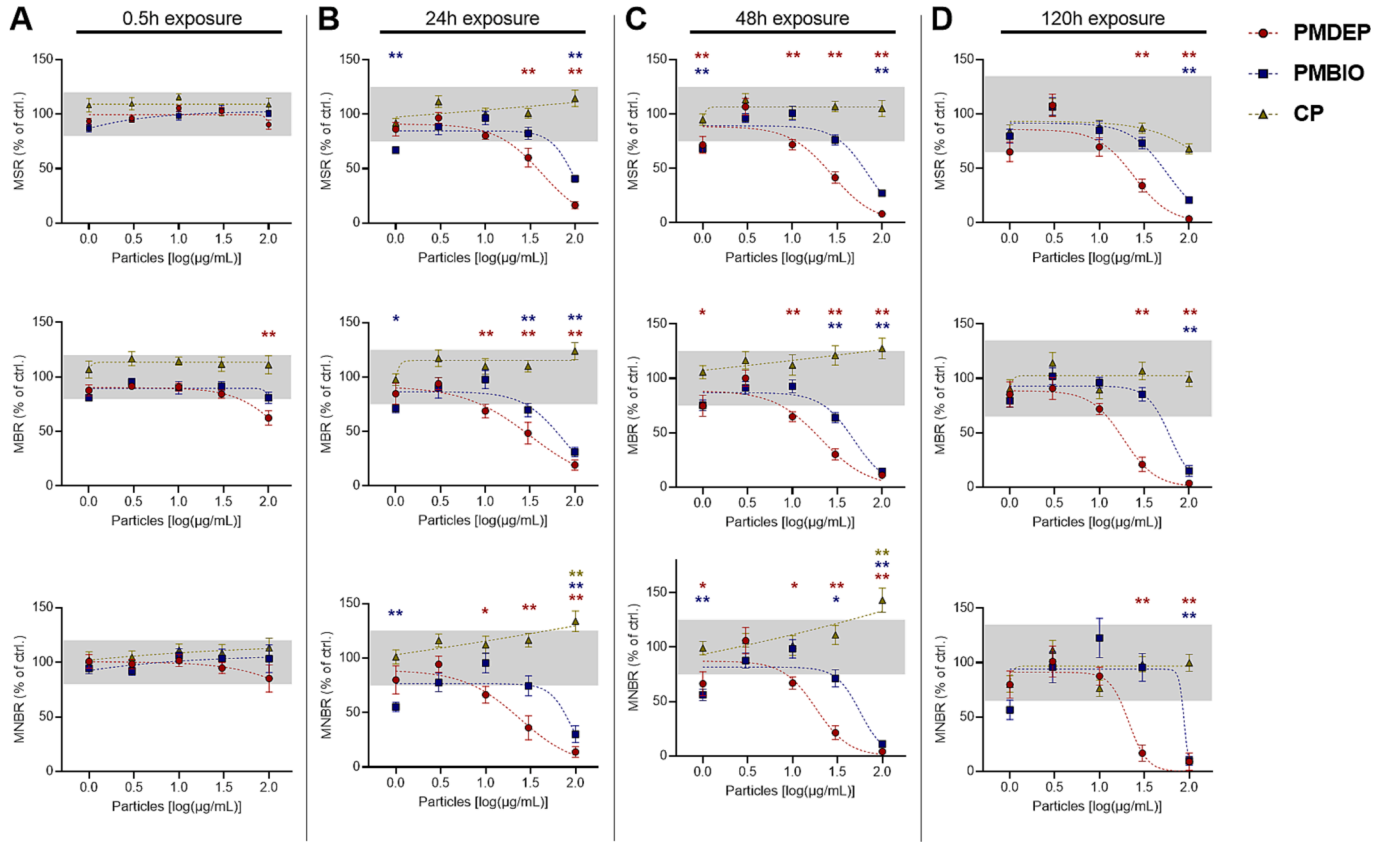

Fig. 8. Changes in neuronal activity following direct exposure to PMDEP (red circles), PMBIO (blue squares), or CP (green triangles). Neuronal activity, presented as mean spike rate (MSR; top), mean burst rate (MBR; middle), and mean network burst rate (MNBR; bottom) was recorded after 0.5 h (**A**), 24 h (**B**), 48 h (**C**), and 120 h (**D**) exposure. Data are depicted as mean treatment ratio (±SEM) in % of control from $n = 18–24$ wells, $N = 3$ plates. Dose-response curves (dashed lines) were computed and indicated in the graphs. Grey area indicates biological variation of MEA data (based on SD of time-matched controls), which is used as a benchmark for toxicological relevance: 0.5 h: 20 %, 24 h: 25 %, 48 h: 25 %, and 120 h: 35 %. * $p < 0.05$ compared to control and exceeding the benchmark response level (grey area), ** $p < 0.01$ compared to control and exceeding the benchmark response level (grey area). (For interpretation of the references to colour in this figure legend, the reader is referred to the web version of this article.)

control) without affecting metabolic activity (Fig. S6). However, overall, TNF-α exhibited only minor (inhibitory) effects on neuronal activity of rat primary cortical cells following direct exposure.

4. Discussion

We studied for the first time the effect of diesel engine combustion-

Table 2
In vitro benchmark dose levels (±upper and lower limit of 95 % confidence interval) for inhibition of neuronal activity by PMDEP and PMBIO after acute (0.5 h) and prolonged (24 h, 48 h, and 120 h) exposure. *In vitro* benchmark dose level were assessed from *in vitro* neurotoxicity screening in rat primary cortical cells and are expressed in μg/mL. Benchmark response levels are defined based on the SD of time-matched control, i.e. 20 %, 25 %, and 35 % for 0.5 h, 24 h and 48 h, and 120 h, respectively. N.A., not applicable (could not be determined); MSR, mean spike rate; MBR, mean burst rate; MNBR, mean network burst rate.

Sample ID	Neuronal activity parameter	Exposure duration			
		0.5 h	24 h	48 h	120 h
PMDEP	MSR	120 [106 – 262]	14 [8.1 – 22]	9.2 [5.5 – 14]	11 [7.4 – 17]
	MBR	52 [26 – 84]	4.7 [1.7 – 10]	9.7 [4.4 – 17]	14 [8.6 – 22]
	MNBR	78 [37 – 110]	9 [3.0 – 20]	11 [5.7 – 20]	16 [9.7 – 21]
PMBIO	MSR	N.A.	62 [44 – 84]	42 [30 – 60]	41 [28 – 60]
	MBR	260 [16 – >100,000]	35 [20 – 56]	27 [19 – 37]	51 [35 – 72]
	MNBR	N.A.	48 [26 – 75]	36 [23 – 64]	62 [38 – 61]

derived PM2.5 on neuronal function *in vitro,* which complements the existing data on (neuro)toxicity evoked by PMDEP and PMBIO. Moreover, we applied a novel approach to investigate the indirect effects of particles on neuronal function and health upon simulated inhalation exposure and thereby incorporated the systemic exposure route and secondary exposure effect. Finally, by comparing the neurotoxic potency of PMDEP and PMBIO, our study provides important toxicity data for risk assessors and regulators to evaluate the possible reduction in human health hazard by replacing petroleum-based diesel with biodiesel fuel.

We demonstrated that simulated inhalation exposure to diesel combustion-derived PM can induce modest effects on neuronal function, while effects on lung cells are virtually absent. In the Calu-3-TDM co-culture lung model, PM or CP did not cause cytotoxicity, barrier disruption or inflammation in the dose range tested (Figs. 2–4). The overall lack of toxicity in our *in vitro* lung model following exposure to PMDEP is partly in line with previous reports where non-cytotoxic doses of diesel exhaust PM did not disrupt cellular morphology, indicative of barrier integrity, nor increased the level of cytokines in basal media (Klein et al., 2017; Steiner et al., 2015, 2013). Further, although the time point used in our study to measure cytokine levels (after 48 h exposure) may be suboptimal given the possible degradation or re-uptake of cytokines, our findings seem to be largely in line with a recent study exposing a co-culture of A549 cells and TDMs to fresh diesel exhaust PM.

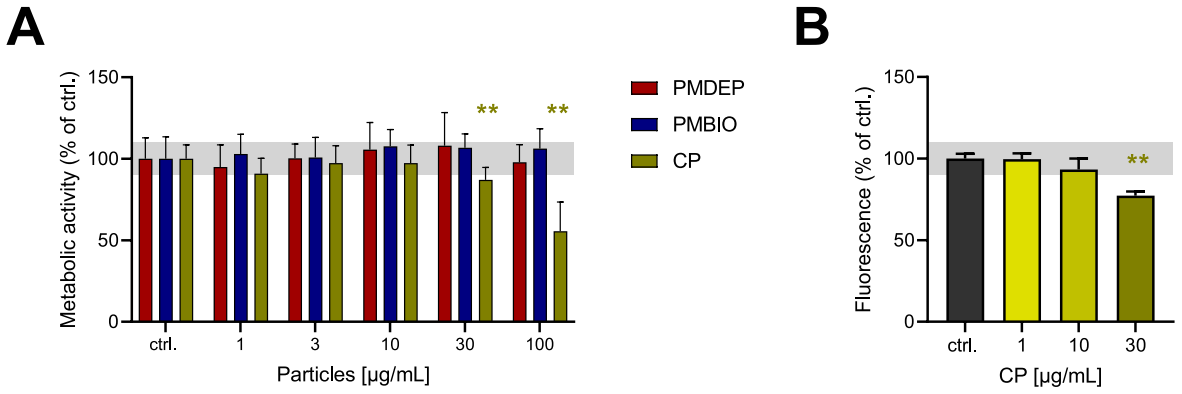

Fig. 9. Metabolic activity of the *in vitro* brain model following direct exposure to PMDEP (red), PMBIO (blue) or CP (green). **A)** Metabolic activity of rat primary cortical cultures after 120 h exposure is depicted as mean (±SD) in % of control from $n = 18–24$ wells, $N = 3$ plates. Grey area indicates 90 %–110 % cell viability (SD of control), which is used as a threshold for relevant changes in cell viability. **B)** Assessment of CP interference with the fluorescent signal of resorufin. Fluorescence was measured with 1–30 μg/mL CP and data is presented as mean (±SD) in % of control (pure resorufin) from $n = 3$ wells, $N = 1$ experiment. ** $p < 0.01$ compared to control and exceeding the benchmark response level (grey area). (For interpretation of the references to colour in this figure legend, the reader is referred to the web version of this article.)

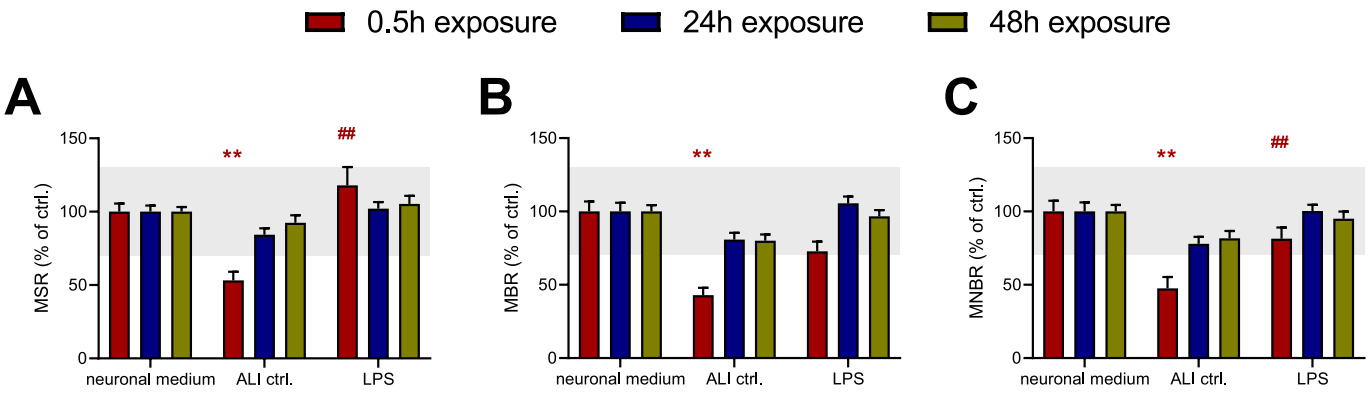

Fig. 10. Modulation of neuronal activity of rat primary cortical cells following simulated inhalation exposure to LPS. Neuronal activity, presented as mean spike rate (MSR; A), mean burst rate (MBR; B), or mean network burst rate (MNBR; C), was recorded after 0.5 h, 24 h, and 48 h exposure. Data are depicted as mean treatment ratio (±SEM) in % of neuronal medium control from $n = 30–32$ wells, $N = 4$ plates. Effects ≤ 30 % (based on SD of neuronal medium control) are considered to be of limited toxicological relevance and indicated by the grey area. ** $p < 0.01$ compared to time-matched neuronal medium control; # $p < 0.05$ compared to time-matched ALI ctrl medium; ## $p < 0.01$ compared to time-matched ALI ctrl medium..

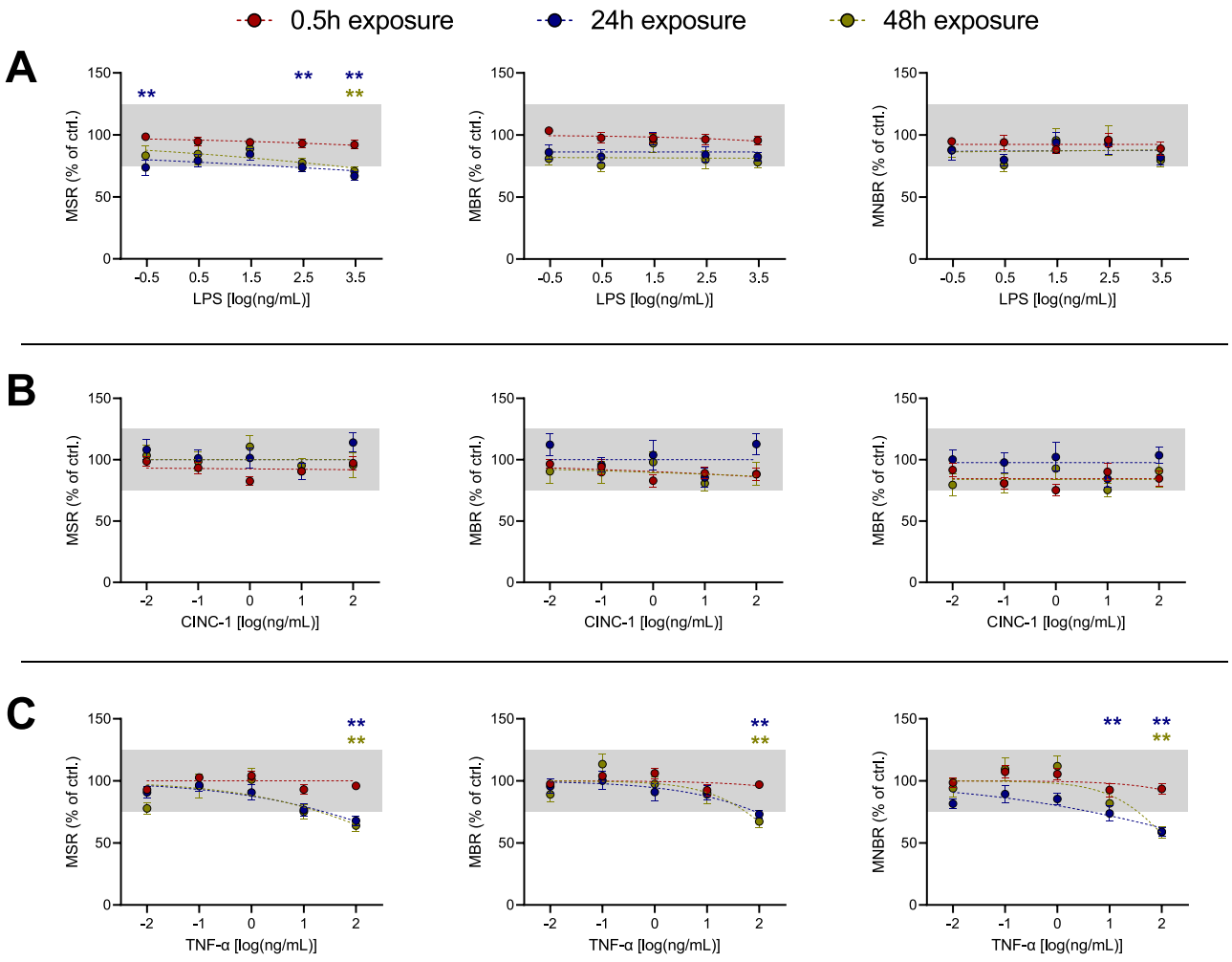

Fig. 11. Modulation of neuronal activity of rat primary cortical cells following direct exposure to LPS (A), CINC-1 (B), and TNF-α (C). Neuronal activity, presented as mean spike rate (MSR; left) mean burst rate (MBR; middle), and mean network burst rate (MNBR; right), was recorded after 0.5 h, 24 h, and 48 h exposure. Data are depicted as mean treatment ratio (±SEM) in % of control from $n = 14$–16 wells, $N = 2$ plates. Effects ≤ 25 % (the SD of control) are considered to be of limited toxicological relevance and indicated by the grey area. * $p < 0.05$ compared to time-matched control and exceeding grey area; ** $p < 0.01$ compared to time-matched control and exceeding grey area.

Here, 24 h post exposure, non-cytotoxic dose of diesel exhaust PM (4.2 ng/cm^2) decreased secretion of IL-6, IL-1β, and TNF-α into the media, whereas IL-8 secretion was unaffected (Hakkarainen et al., 2023). Such a decrease would not be expected in lung cells where usually the opposite response it noted. Importantly, the exposure dose is relatively low compared to studies reporting an increase in cytokine secretion, and the authors linked the decreased cytokine levels following diesel exhaust PM exposure with an immunosuppressive effect (Hakkarainen et al., 2023).

The gene expression analysis of the lung model exposed to PM suggest only minor signs of cell stress and oxidative stress (Fig. 5). Increased gene expression was especially observed in inserts exposed to PMDEP and PMBIO for CYP1A1 which is in line with previous findings in BEAS-2B cells (Totlandsdal et al., 2010). Totlandsdal and colleagues (2010) reported that diesel exhaust particles (≈ 4–40 ng/cm^2) induce CYP1A1 expression. Interestingly, the activation of proinflammatory pathways indicated by increased expression of IL-6, IL-8 and COX-2 was only observed at much higher doses (≈ 16 μg/cm^2; Totlandsdal et al., 2010), possibly explaining why cytokine levels remained unaffected in our study.

Interestingly, in our study, the expression of mRNA associated with cell stress (CYP1A1) and oxidative stress (GPX) appeared to be more prominent following PMBIO exposure. This is in line with the results of a recent study where human primary bronchial epithelial cells were exposed to PM from fossil diesel or from biodiesel blends of different ratios (20 %, 50 %, 100 %) using fatty acid methyl esters FAME (soy bean methyl ester) (Ogbunuzor et al., 2023). While the fold increase in CYP1A1 expression was comparable following exposure to PM from fossil diesel and 20 % biodiesel blend, increasing FAME ratio resulted in increased expression of several stress response genes (CYP1A1, NQO1 and IL-1β) indicating higher potency of FAME (Ogbunuzor et al., 2023) to induce genes involved in the bioactivation of polycyclic aromatic hydrocarbons (PAHs). Further, in BEAS-2B cells, PM derived from the same biodiesel blend as used in our study exhibited higher cytotoxicity than PM from fossil diesel, and caused IL-6 secretion after 24 h submerged exposure (Gerlofs-Nijland et al., 2013). The absence of cytokine release and cytotoxicity in our study is likely due to differences in lung models, dose levels and exposure methods (submerged vs ALI). On the other hand, studies using RAW264.7 macrophages or a triple culture *in vitro* lung model indicate that the supplementation of gasoline with (bio) ethanol may reduce cytotoxicity and oxidative potential (Bisig et al., 2016; Hakkarainen et al., 2020). Together, these results emphasize the importance of the type and composition of biofuels (FAME vs bio-ethanol), blending ratio, and engine technology for the hazard of emitted PM (Kousoulidou, et al., 2012; Landwehr et al., 2023).

Direct exposure of rat primary cortical cultures to PMDEP and PMBIO dose-dependently inhibited neuronal activity following 24–120

h exposure (Fig. 8B–C), which is not the result of cytotoxicity (Fig. 9). The absence of cytotoxicity at the applied doses (1–100 μg/mL) is in line with previous reports where 24 h exposure of rat primary neuron-glia cultures to 200 μg/mL diesel exhaust particles (Kim et al., 2022) or of murine dopaminergic neurons to 100 μg/mL (Roqué et al., 2016) did also not cause cytotoxicity. Based on our neurotoxicity data, PMDEP has a higher neurotoxic potency than PMBIO, with lowest effect levels of 10 μg/mL and 30 μg/mL, respectively (Fig. 8, Table 2, Fig. S5) assuming equal PM deposition rates.

Evaluation of the physiological relevance of this dose-dependent effect remains challenging as internal dose levels (brain levels) of PM upon *in vivo* inhalation or nasal instillation are unknown. Consequently, the *in vitro* dose cannot be extrapolated to an external exposure, thereby hampering further risk assessment. Although direct neurotoxicity aims to resemble brain exposure via the olfactory route, the highest doses of PM are likely found in olfactory structures and not in the cortex. Importantly, cell types vary between different brain structures, thereby likely also affecting the PM effect and toxicity. Besides, interspecies differences regarding toxicodynamics may apply. Previous research demonstrated that depending on the test compound, neuronal activity of rat primary cortical cultures is comparable to or even more sensitive than those of human induced pluripotent stem cells (hiPSC)-derived neuronal cultures (Kasteel and Westerink, 2017; Hondebrink et al., 2017). Notably, though, for hazard characterization and potency ranking of PM2.5 from different fuels, the rat cortical culture is an adequate model to compare neurotoxic potencies.

Interestingly, the reduction of neuronal activity following direct acute exposure (0.5 h) is very limited (Fig. 8A), which may be the result of a relative low deposited dose. We have previously reported that following 0.5 h exposure to titanium dioxide and silver nanoparticle suspensions (primary particle size: 26–40 nm; mode diameter of agglomerated: 200–400 nm) only 0.5–0.7 % of the total particle mass is deposited on the cells (Gerber et al., 2022). Also for PM and CP the nominal dose delivered to the cells is likely minimal, which would thus limit physical interaction of PM with the cortical culture, thereby possibly explaining the delayed effect. Alternatively, the lack of acute effects suggests that the inhibition following prolonged exposure is likely not due to immediate interaction of the PM with for example neurotransmitter receptors or ion channels, but rather to indirect effects. It may very well be that the inhibition of neuronal activity is due to indirect processes, like release of cellular mediator as cytokines (besides CINC-1 and TNF-α), accumulation of ROS, and/or changes in gene expression. However, elucidation of the exact modes of action is challenging due to the complex composition of PMDEP and PMBIO and should be further explored in follow up studies. It should be noted that conditions during PM generation, e.g., engine type, fuel type, filter material, have a critical impact on the composition of the PM samples and their toxicity (Bengalli et al., 2019), which further hampers elucidation of the mechanisms as well as comparison with other studies. Nevertheless, the current data clearly demonstrate that PMBIO and particularly PMDEP exhibit neurotoxic potency.

In contrast to the significant and dose-dependent neurotoxicity following direct exposure, simulated inhalation exposure via PM-medium collected from the lung model caused a transient and modest increase in the neuronal activity of the primary cortical cells during acute exposure (Fig. 6). Particle translocation across the *in vitro* lung model depends on the formed cell barrier, the size of the particles and the membrane on which the lung cells were grown, especially the membrane pore size. Overall, it remains unclear if and to what extend the combustion-derived particles and chemicals released from their surface have reached the basolateral compartment for subsequent interaction with the neuronal cell cultures. Importantly, the inclusion of the lung model results in opposite effects on neuronal function following simulated inhalation exposure compared to direct exposure to PMDEP and PMBIO. Therefore, the acute changes in neuronal activity following simulated inhalation exposure could not be caused by translocated particles or adsorbed chemicals.

Notably, a comparable increase in MSR and MNBR as seen for PMBIO and partly for PMDEP following simulated inhalation exposure was also observed following exposure to medium from LPS-exposed lung cells (Fig. 10). However, no elevated cytokine levels were detected in the basal medium from PMDEP- and PMBIO-exposed inserts (Fig. 4) and the direct exposure of rat cortical cultures to LPS or cytokines did not increase neuronal activity (Fig. 11). Therefore, the neuromodulatory effect following simulated inhalation exposure is unlikely due to released cytokines in the basal medium. Our combined findings indicate that the lung can act as an efficient barrier for the inhibitory components in the PM samples and suggests that the *in vitro* lung model releases factors with neuromodulatory properties. Although the neuromodulatory factors secreted by the lung model and the underlying causes remain to be identified, these findings highlight the need for additional research using integrated readouts and cell models.

Our study consistently shows that CP cause only minor (neuro)toxic effects in comparison to PMDEP and PMBIO. Neither did CP inhibit neuronal activity following direct exposure nor did CP-medium from the lung model cause transient increase of neuronal activity in rat primary cortical cells. This lack of toxic effects of CP suggests that the (neuro) toxicity of PMDEP and PMBIO is caused by combustion-derived chemicals on the surface of the PM, e.g., metals or organic carbons including PAH, n-alkanes, and that it is not due to the clean carbon core. This conclusion is in line with previous studies where (geno)toxic potential and the immune response of PM from diesel (and biodiesel) exhaust were clearly related to the adsorbed chemicals (Hakkarainen et al., 2022; Ogbunuzor et al., 2023).

In vitro models can have shortcomings that should be taken into account when interpreting the data. Notably, Calu-3 cells form a very strong barrier (TEER $> 1000\ \Omega/cm^2$), which is much stronger than the barrier of other lung epithelial cell lines (He et al., 2021) and may even be stronger than in the *in vivo* situation. It is further important to note that the transwell membrane (0.4 μm pore size) may hamper particles from translocating into the basolateral compartment. Moreover, the absence of inhibition of neuronal activity following simulated inhalation exposure may be related to the relatively low exposure range compared to the doses used for direct exposure. Although the highest applied dose in the *in vitro* lung model was 3.9 $\mu g/cm^2$, the PM concentration in the basal medium after 48 h was maximal 4.4 μg/mL (based on 1.12 cm^2 per membrane, 1 mL medium in the basolateral compartment and assuming 100 % translocation). With the technically required dilution step from the *in vitro* lung model to the *in vitro* brain model, the maximal PM dose to which neuronal cultures were exposed could not have exceeded 1.1 μg/mL. Since the lowest observed effect level for direct exposure of the cortical culture amounts to 10 μg/mL and 30 μg/mL for respectively PMDEP and PMBIO it is thus not very surprising that the possible effects of the PM remain undetected. Unfortunately, there are practical limitations preventing higher exposure levels including limited availability of generated PM2.5 sample, whereas higher exposure levels would also result in unrealistic high dose (rates). So, while the inclusion of an *in vitro* lung model may make the exposure route more relevant to the *in vivo* situation, it also limits the maximal exposure levels for the brain model and thereby hampers further hazard characterization.

The combination of the lung model with neurotoxicity screening aims to simulate the systemic exposure route of PM2.5 upon inhalation. While our approach includes a lung-blood barrier represented by the ALI lung model, several additional cell types and structures that may play a crucial role in the systemic exposure effect of particles are lacking. The most important ones are the endothelial and blood–brain barrier, which may get disrupted by particles and further promote systemic and neuroinflammation. Regarding the limitations of the *in vitro* brain model per se, rat primary cortical cultures consist of multiple cell types, including neuronal and glia cells, e.g. astrocytes. Especially microglia may be of great importance for the neurotoxicity of PM as neuroinflammation and microglia activation has been reported by several research groups

(Shkirkova et al., 2022; Ha et al., 2022; Cole et al., 2016; Durga et al., 2015; Gerlofs-Nijland et al., 2010; Levesque et al., 2011; Lucchini et al., 2012). However, the proportion of microglia in rat cortical cultures (derived at PND0-1) is very low, likely explaining the limited response of the brain model towards the inflammatory stimuli like LPS and cytokines.

Finally, while direct exposure of rat primary cortical cells caused a clear dose-dependent decrease of neuronal activity, other endpoints assessed in our study did not show such a clear relationship, i.e. gene expression in the *in vitro* lung model and indirect neurotoxicity in the *in vitro* brain model. For the first, the limited number of replicates and a possibly unequal deposition of the nebulized PM may cause/contribute to the absence of a dose–response relationship. For the latter, exposure to medium form an independently exposed *in vitro* model is not representing a defined dose range as is the case for a direct exposure. The effective mediators released by the *in vitro* lung model may differ per PM dose as different pathways may be activated depending on the dose, highlighting the complexity and challenges that need to be taken into account when studying cell–cell interaction and secondary toxicity *in vitro*.

It is important to consider that in real-life, exposure to PMDEP and PMBIO will occur simultaneously. As the aim of this study was to shed light on the impact of further supplementation of fossil diesel with FAME on the neurotoxic potency, the PM samples were only studied independently and not in a mixture scenario. Thus, our data cannot rule out that the more complex real-life exposure to fuel combustion that includes additional pollutants, e.g. gases, is more potent than the PM2.5 fraction alone. Moreover, a reduction of PM hazard does not necessarily decrease the risk of engine emissions-derived PM for human health. The application of biofuel has been reported to effectively reduce PAH and PM emissions in the exhaust of fossil diesel (Tan et al., 2009; Traviss et al., 2010; Ogbunuzor et al., 2023). Nevertheless, the chemical composition of the exhaust emission highly depends on the origin of the FAME, blending ratio and engine technology which in turn critically determines the hazard of the PM (Kousoulidou, et al., 2012; Landwehr et al., 2023). Furthermore, previous studies found that the oxidative potential of biodiesel-derived PM is decreased when expressed on a per kilometer basis even though per unit mass they exhibit higher oxidative potency than PM from regular diesel fuel (Kooter et al., 2011; Cheung et al., 2009; Gerlofs-Nijland et al., 2013), highlighting the importance of assessing PM emission.

5. Conclusion

In summary, the results presented here provide important insights into the toxic potency of PMDEP, PMBIO and CP. Effects of 48 h exposure on a lung model are limited to upregulation of genes indicative for (modest) oxidative and cell stress. While the transient neurotoxic effects of simulated inhalation exposure are modest, clear neurotoxic effects are observed following prolonged direct exposure to PM, with PMDEP being more potent in inhibiting neuronal activity compared to PMBIO. Given the lack of effect for CP exposure, our data suggest that the neurotoxic effects of engine emission-derived PM are caused by adsorbed chemicals rather than the pure carbon core.

CRediT authorship contribution statement

Lora-Sophie Gerber: Writing – review & editing, Writing – original draft, Visualization, Methodology, Investigation, Formal analysis, Conceptualization. **Dirk C.A. de Leijer:** Investigation, Formal analysis. **Andrea Rujas Arranz:** Formal analysis, Investigation. **Jonas M.M.L. Lehmann:** Formal analysis, Investigation. **Meike E. Verheul:** Investigation, Formal analysis. **Flemming R. Cassee:** Conceptualization, Methodology, Writing – review & editing, Supervision, Project administration, Funding acquisition. **Remco H.S. Westerink:** Conceptualization, Methodology, Writing – review & editing, Supervision, Project administration, Funding acquisition.

Declaration of competing interest

The authors declare that they have no known competing financial interests or personal relationships that could have appeared to influence the work reported in this paper.

Data availability

Data will be made available on request.

Acknowledgements

We gratefully acknowledge Evert Duistermaat and Daan Leseman from the National Institute for Public Health and the Environment (RIVM; the Netherlands) for their great technical support and Jolanda Vermeulen and Eric Gremmer from the National Institute for Public Health and the Environment (RIVM; the Netherlands) for their help with cell culturing THP-1 and Calu-3 cells. Further, we gratefully acknowledge Tobias Pfeiffer from VSPARTICLE and Pasi I. Jalava from the University of Eastern Finland for providing the clean carbon particles and the members of the Neurotoxicology Research Group (Utrecht University) for valuable discussions. This work has been funded by the European Union's Horizon 2020 research and innovation programme under grant agreement No 814978 (TUBE), the National Institute for Public Health and the Environment (RIVM, The Netherlands), and the Faculty of Veterinary Medicine (Utrecht University, The Netherlands). The authors declare they have no competing financial interests.

Appendix A. Supplementary data

Supplementary data to this article can be found online at https://doi.org/10.1016/j.envint.2024.108481.

References

Aquino, G.V., Dabi, A., Odom, G.J., Lavado, R., Nunn, K., Thomas, K., Schackmuth, B., Shariff, N., Jarajapu, M., Pluto, M., Miller, S.R., Eller, L., Pressley, J., Patel, R.R., Black, J., Bruce, E.D., 2023. Evaluating the effect of acute diesel exhaust particle exposure on P-glycoprotein efflux transporter in the blood-brain barrier co-cultured with microglia. Curr Res Toxicol. 4 https://doi.org/10.1016/j.crtox.2023.100107.

Bengalli, R., Zerboni, A., Marchetti, S., Longhin, E., Priola, M., Camatini, M., Mantecca, P., 2019. In vitro pulmonary and vascular effects induced by different diesel exhaust particles. Toxicol. Lett. 306, 13–24. https://doi.org/10.1016/J.TOXLET.2019.01.017.

Bisig, C., Roth, M., Müller, L., Comte, P., Heeb, N., Mayer, A., Czerwinski, J., Petri-Fink, A., Rothen-Rutishauser, B., 2016. Hazard identification of exhausts from gasoline-ethanol fuel blends using a multi-cellular human lung model. Environ. Res. 151, 789–796. https://doi.org/10.1016/j.envres.2016.09.010.

Bongaerts, E., Lecante, L.L., Bové, H., Roeffaers, M.B.J., Ameloot, M., Fowler, P.A., Nawrot, T.S., 2022. Maternal exposure to ambient black carbon particles and their presence in maternal and fetal circulation and organs: an analysis of two independent population-based observational studies. The Lancet Planet Health., 6, e804-e811. https://doi: 10.1016/S2542-5196(22)00200-5.

Braakhuis, H.M., Gosens, I., Krystek, P., Boere, J.A.F., Cassee, F.R., Fokkens, P.H.B., Post, J.A., van Loveren, H., Park, M.V.D.Z., 2014. Particle size dependent deposition and pulmonary inflammation after short-term inhalation of silver nanoparticles. Part. Fibre Toxicol. 11 https://doi.org/10.1186/s12989-014-0049-1.

Braakhuis, H.M., He, R., Vandebriel, R.J., Gremmer, E.R., Zwart, E., Vermeulen, J.P., Fokkens, P., Boere, J., Gosens, I., Cassee, F.R., 2020. An air-liquid interface bronchial epithelial model for realistic, repeated inhalation exposure to airborne particles for toxicity testing. J. vis. Exp. 2020, 61210. https://doi.org/10.3791/61210.

Cacciottolo, M., Wang, X., Driscoll, I., Woodward, N., Saffari, A., Reyes, J., Serre, M.L., Vizuete, W., Sioutas, C., Morgan, T.E., Gatz, M., Chui, H.C., Shumaker, S.A., Resnick, S.M., Espeland, M.A., Finch, C.E., Chen, J.C., 2017. Particulate air pollutants, APOE alleles and their contributions to cognitive impairment in older women and to amyloidogenesis in experimental models. Transl. Psychiatry 7, e1022–e. https://doi.org/10.1038/tp.2016.280.

Calderón-Garcidueñas, L., Ayala, A., 2022. Air Pollution, Ultrafine Particles, and Your Brain: Are Combustion Nanoparticle Emissions and Engineered Nanoparticles Causing Preventable Fatal Neurodegenerative Diseases and Common Neuropsychiatric Outcomes? Environ. Sci. Technol. https://doi.org/10.1021/acs.est.1c04706.

Carvalho, T.C., Peters, J.I., Williams, R.O., 2011. Influence of particle size on regional lung deposition - What evidence is there? Int. J. Pharm. https://doi.org/10.1016/j.ijpharm.2010.12.040.

Cassee, F.R., Fokkens, P.H.B., Leseman, D.L.A.C., Bloemen, H.J.T., Boere, A.J.F., 2003. Respiratory allergy and inflammation due to ambient particles (RAIAP). Collection and characterisation of particulate matter samples from five European sites, RIVM report http://www.rivm.nl/bibliotheek/rapporten/863001001.

Cassee, F.R., Héroux, M.E., Gerlofs-Nijland, M.E., Kelly, F.J., 2013. Particulate matter beyond mass: Recent health evidence on the role of fractions, chemical constituents and sources of emission. Inhal. Toxicol. https://doi.org/10.3109/08958378.2013.850127.

Cheung, K.L., Polidori, A., Ntziachristos, L., Tzamkiozis, T., Samaras, Z., Cassee, F.R., Gerlofs, M., Sioutas, C., 2009. Chemical characteristics and oxidative potential of particulate matter emissions from gasoline, diesel, and biodiesel cars. Environ. Sci. Technol. 43 https://doi.org/10.1021/es900819t.

Cole, T.B., Coburn, J., Dao, K., Roqué, P., Chang, Y.C., Kalia, V., Guilarte, T.R., Dziedzic, J., Costa, L.G., 2016. Sex and genetic differences in the effects of acute diesel exhaust exposure on inflammation and oxidative stress in mouse brain. Toxicology 374, 1–9. https://doi.org/10.1016/J.TOX.2016.11.010.

Costa, L.G., Cole, T.B., Coburn, J., Chang, Y.C., Dao, K., Roque, P.J., 2017. Neurotoxicity of traffic-related air pollution. Neurotoxicology 59, 133–139. https://doi.org/10.1016/j.neuro.2015.11.008.

Costa, L.G., Cole, T.B., Dao, K., Chang, Y.C., Coburn, J., Garrick, J., 2019. Neurotoxicity of air pollution: Role of neuroinflammation. In: Advances in Neurotoxicology. Academic Press, pp. 195–221. https://doi.org/10.1016/bs.ant.2018.10.007.

Costa, L.G., Cole, T.B., Coburn, J., Chang, Y.C., Dao, K., Roque, P.J., 2014. Neurotoxicants are in the air: Convergence of human, animal, and in vitro studies on the effects of air pollution on the brain. Biomed Res. Int. https://doi.org/10.1155/2014/736385.

Dingemans, M.M.L., Schütte, M.G., Wiersma, D.M.M., de Groot, A., van Kleef, R.G.D.M., Wijnolts, F.M.J., Westerink, R.H.S., 2016. Chronic 14-day exposure to insecticides or methylmercury modulates neuronal activity in primary rat cortical cultures. Neurotoxicology 57, 194–202. https://doi.org/10.1016/j.neuro.2016.10.002.

Donaldson, K., Tran, L., Jimenez, L.A., Duffin, R., Newby, D.E., Mills, N., MacNee, W., Stone, V., 2005. Combustion-derived nanoparticles: A review of their toxicology following inhalation exposure. Part. Fibre Toxicol. https://doi.org/10.1186/1743-8977-2-10.

Durga, M., Devasena, T., Rajasekar, A., 2015. Determination of LC50 and sub-chronic neurotoxicity of diesel exhaust nanoparticles. Environ. Toxicol. Pharmacol. 40, 615–625. https://doi.org/10.1016/j.etap.2015.06.024.

Elder, A., Gelein, R., Silva, V., Feikert, T., Opanashuk, L., Carter, J., Potter, R., Maynard, A., Ito, Y., Finkelstein, J., Oberdörster, G., 2006. Translocation of inhaled ultrafine manganese oxide particles to the central nervous system. Environ. Health Perspect. 114, 1172–1178. https://doi.org/10.1289/ehp.9030.

Gerber, L.S., Heusinkveld, H.J., Langendoen, C., Stahlmecke, B., Schins, R.P., Westerink, R.H., 2022. Acute, sub-chronic and chronic exposures to TiO2 and Ag nanoparticles differentially affects neuronal function in vitro. Neurotoxicology 93, 311–323. https://doi.org/10.1016/j.neuro.2022.10.010.

Gerber, L.-S., van Melis, L.V.J., van Kleef, R.G.D.M., de Groot, A., Westerink, R.H.S., 2021. Culture of Rat Primary Cortical Cells for Microelectrode Array (MEA) Recordings to Screen for Acute and Developmental Neurotoxicity. Curr. Protoc. 1, e158.

Gerlofs-Nijland, M.E., van Berlo, D., Cassee, F.R., Schins, R.P.F., Wang, K., Campbell, A., 2010. Effect of prolonged exposure to diesel engine exhaust on proinflammatory markers in different regions of the rat brain. Part. Fibre Toxicol. 7 https://doi.org/10.1186/1743-8977-7-12.

Gerlofs-Nijland, M.E., Totlandsdal, A.I., Tzamkiozis, T., Leseman, D.L.A.C., Samaras, Z., Låg, M., Schwarze, P., Ntziachristos, L., Cassee, F.R., 2013. Cell toxicity and oxidative potential of engine exhaust particles: Impact of using particulate filter or biodiesel fuel blend. Environ. Sci. Technol. 47, 5931–5938. https://doi.org/10.1021/es305330y.

Ha, S.M., Barnhill, L.M., Li, S., Bornstein, J.M., 2022. Neurotoxicity of diesel exhaust extracts in zebrafish and its implications for neurodegenerative disease. Sci Rep. 12, 19371. https://doi.org/10.1038/s41598-022-23485-2.

Hakkarainen, H., Aakko-Saksa, P., Sainio, M., Ihantola, T., Rönkkö, T.J., Koponen, P., Rönkkö, T., Jalava, P.I., 2020. Toxicological evaluation of exhaust emissions from light-duty vehicles using different fuel alternatives in sub-freezing conditions. Part. Fibre Toxicol. 17, 1–17. https://doi.org/10.1186/S12989-020-00348-0/FIGURES/7.

Hakkarainen, H., Salo, L., Mikkonen, S., Saarikosko, S., Aurela, M., Teinilä, K., Ihalainen, M., Martikainen, S., Marjanen, P., Lepistö, T., Kuittinen, N., Saarnio, K., Aakko-Saksa, P., Pfeiffer, T.V., Timonen, H., Rönkkö, T., Jalava, P.I., 2022. Black carbon toxicity dependence on particle coating: Measurements with a novel cell exposure method. Sci. Total Environ. 838 https://doi.org/10.1016/j.scitotenv.2022.156543.

Hakkarainen, H., Järvinen, A., Lepistö, T., Salo, L., Kuittinen, N., Laakkonen, E., Yang, M., Martikainen, M.V., Saarikoski, S., Aurela, M., Barreira, L., Teinilä, K., Ihalainen, M., Aakko-Saksa, P., Timonen, H., Rönkkö, T., Jalava, P., 2023. Toxicity of exhaust emissions from high aromatic and non-aromatic diesel fuels using in vitro ALI exposure system. Sci. Total Environ. 890, 164215 https://doi.org/10.1016/J.SCITOTENV.2023.164215.

He, R.W., Gerlofs-Nijland, M.E., Boere, J., Fokkens, P., Leseman, D., Janssen, N.A.H., Cassee, F.R., 2020. Comparative toxicity of ultrafine particles around a major airport in human bronchial epithelial (Calu-3) cell model at the air–liquid interface. Toxicol. Vitr. 68, 104950 https://doi.org/10.1016/j.tiv.2020.104950.

He, R.W., Braakhuis, H.M., Vandebriel, R.J., Staal, Y.C.M., Gremmer, E.R., Fokkens, P.H.B., Kemp, C., Vermeulen, J., Westerink, R.H.S., Cassee, F.R., 2021. Optimization of an air-liquid interface in vitro cell co-culture model to estimate the hazard of aerosol exposures. J. Aerosol Sci. 153, 105703 https://doi.org/10.1016/J.JAEROSCI.2020.105703.

Heusinkveld, H.J., Wahle, T., Campbell, A., Westerink, R.H.S., Tran, L., Johnston, H., Stone, V., Cassee, F.R., Schins, R.P.F., 2016. Neurodegenerative and neurological disorders by small inhaled particles. Neurotoxicology 56, 94–106. https://doi.org/10.1016/j.neuro.2016.07.007.

Hondebrink, L., Kasteel, E.E.J., Tukker, A.M., Wijnolts, F.M.J., Verboven, A.H.A., Westerink, R.H.S., 2017. Neuropharmacological characterization of the new psychoactive substance methoxetamine. Neuropharmacology. 123, 1–9. https://doi:10.1016/j.neuropharm.2017.04.035.

Hullmann, M., Albrecht, C., van Berlo, D., Gerlofs-Nijland, M.E., Wahle, T., Boots, A.W., Krutmann, J., Cassee, F.R., Bayer, T.A., Schins, R.P.F., 2017. Diesel engine exhaust accelerates plaque formation in a mouse model of Alzheimer's disease. Part. Fibre Toxicol. 14 https://doi.org/10.1186/s12989-017-0213-5.

Ishihara, Y., Kagawa, J., 2003. Chronic diesel exhaust exposures of rats demonstrate concentration and time-dependent effects on pulmonary inflammation. Inhal. Toxicol. 15, 473–492. https://doi.org/10.1080/08958370304464.

Johnstone, A.F.M., Gross, G.W., Weiss, D.G., Schroeder, O.H.U., Gramowski, A., Shafer, T.J., 2010. Microelectrode arrays: A physiologically based neurotoxicity testing platform for the 21st century. Neurotoxicology. 31 (4) https://doi.org/10.1016/j.neuro.2010.04.001.

Karagulian, F., Belis, C.A., Dora, C.F.C., Prüss-Ustün, A.M., Bonjour, S., Adair-Rohani, H., Amann, M., 2015. Contributions to cities' ambient particulate matter (PM): A systematic review of local source contributions at global level. Atmos. Environ. https://doi.org/10.1016/j.atmosenv.2015.08.087.

Kasteel, E.E., Westerink, R.H., 2017. Comparison of the acute inhibitory effects of Tetrodotoxin (TTX) in rat and human neuronal networks for risk assessment purposes. Toxicol Lett. 15 (270), 12–16. https://doi: 10.1016/j.toxlet.2017.02.014.

Klein, S.G., Cambier, S., Hennen, J., Legay, S., Serchi, T., Nelissen, I., Chary, A., Moschini, E., Krein, A., Blömeke, B., Gutleb, A.C., 2017. Endothelial responses of the alveolar barrier in vitro in a dose-controlled exposure to diesel exhaust particulate matter. Part. Fibre Toxicol. 14 https://doi.org/10.1186/S12989-017-0186-4.

Kooter, I.M., van Vugt, M.A.T.M., Jedynska, A.D., Tromp, P.C., Houtzager, M.M.G., Verbeek, R.P., Kadijk, G., Mulderij, M., Krul, C.A.M., 2011. Toxicological characterization of diesel engine emissions using biodiesel and a closed soot filter. Atmos. Environ. 45 https://doi.org/10.1016/j.atmosenv.2010.12.040.

Kousoulidou, M., Ntziachristos, L., Fontaras, G., Martini, G., Dilara, P., Samaras, Z., 2012. Impact of biodiesel application at various blending ratios on passenger cars of different fueling technologies. Fuel. 98 https://doi.org/10.1016/j.fuel.2012.03.038.

Kreyling, W.G., 2016. Discovery of unique and ENM— specific pathophysiologic pathways: Comparison of the translocation of inhaled iridium nanoparticles from nasal epithelium versus alveolar epithelium towards the brain of rats. Toxicol. Appl. Pharmacol. 299, 41–46. https://doi.org/10.1016/J.TAAP.2016.02.004.

Kuempel, E.D., Sweeney, L.M., Morris, J.B., Jarabek, A.M., 2015. Advances in Inhalation Dosimetry Models and Methods for Occupational Risk Assessment and Exposure Limit Derivation. J. Occup. Environ. Hyg. https://doi.org/10.1080/15459624.2015.1060328.

Landwehr, K.R., Hillas, J., Mead-Hunter, R., King, A., O'Leary, R.A., Kicic, A., Mullins, B. J., Larcombe, A.N., 2023. Biodiesel feedstock determines exhaust toxicity in 20% biodiesel: 80% mineral diesel blends. Chemosphere 310, 136873. https://doi.org/10.1016/j.chemosphere.2022.136873.

Legendy, C.R., Salcman, M., 1985. Bursts and recurrences of bursts in the spike trains of spontaneously active striate cortex neurons. J. Neurophysiol. 53, 926–939. https://doi.org/10.1152/jn.1985.53.4.926.

Levesque, S., Surace, M.J., McDonald, J., Block, M.L., 2011. Air pollution and the brain: Subchronic diesel exhaust exposure causes neuroinflammation and elevates early markers of neurodegenerative disease. J. Neuroinflammation 8. https://doi.org/10.1186/1742-2094-8-105.

Levesque, S., Taetzsch, T., Lull, M.E., Johnson, J.A., McGraw, C., Block, M.L., 2013. The role of MAC1 in diesel exhaust particle-induced microglial activation and loss of dopaminergic neuron function. J. Neurochem. 125, 756–765. https://doi.org/10.1111/jnc.12231.

Li, B., Guo, L., Ku, T., Chen, M., Li, G., Sang, N., 2018. PM2.5 exposure stimulates COX-2-mediated excitatory synaptic transmission via ROS-NF-KB pathway. Chemosphere 190, 124–134. https://doi.org/10.1016/j.chemosphere.2017.09.098.

Lucchini, R.G., Dorman, D.C., Elder, A., Veronesi, B., 2012. Neurological impacts from inhalation of pollutants and the nose-brain connection. Neurotoxicology 33, 838–841. https://doi.org/10.1016/j.neuro.2011.12.001.

Manzetti, S., Andersen, O., 2016. Biochemical and physiological effects from exhaust emissions. A review of the relevant literature. Pathophysiology. https://doi.org/10.1016/j.pathophys.2016.10.002.

McConnell, E.R., McClain, M.A., Ross, J., LeFew, W.R., Shafer, T.J., 2012. Evaluation of multi-well microelectrode arrays for neurotoxicity screening using a chemical training set. Neurotoxicology 33, 1048–1057. https://doi.org/10.1016/j.neuro.2012.05.001.

Miller, M.R., Raftis, J.B., Langrish, J.P., McLean, S.G., Samutrtai, P., Connell, S.P., Wilson, S., Vesey, A.T., Fokkens, P.H.B., Boere, A.J.F., Krystek, P., Campbell, C.J., Hadoke, P.W.F., Donaldson, K., Cassee, F.R., Newby, D.E., Duffin, R., Mills, N.L., 2017. Inhaled Nanoparticles Accumulate at Sites of Vascular Disease. ACS Nano 11, 4542–4552. https://doi.org/10.1021/acsnano.6b08551.

Oberdörster, G., Sharp, Z., Atudorei, V., Elder, A., Gelein, R., Kreyling, W., Cox, C., 2004. Translocation of inhaled ultrafine particles to the brain. Inhal Toxicol. 16, 437–445. https://doi.org/10.1080/08958370490439597.

Oberdörster, G., Elder, A., Rinderknecht, A., 2009. Nanoparticles and the Brain: Cause for Concern? J. Nanosci. Nanotechnol. 9, 4996.

Ogbunuzor, C., Fransen, L.F.H., Talibi, M., Khan, Z., Dalzell, A., Laycock, A., Southern, D., Eveleigh, A., Ladommatos, N., Hellier, P., Leonard, M.O., 2023. Biodiesel exhaust particle airway toxicity and the role of polycyclic aromatic hydrocarbons. Ecotoxicol Environ Saf. 259 https://doi.org/10.1016/j.ecoenv.2023.115013.

Omidvarborna, H., Kumar, A., Kim, D.S., 2015. Recent studies on soot modeling for diesel combustion. Renew. Sustain. Energy Rev. https://doi.org/10.1016/j.rser.2015.04.019.

Peters, R., Ee, N., Peters, J., Booth, A., Mudway, I., Anstey, K.J., 2019. Air Pollution and Dementia: A Systematic Review. J. Alzheimer's Dis. https://doi.org/10.3233/JAD-180631.

Ristovski, Z.D., Miljevic, B., Surawski, N.C., Morawska, L., Fong, K.M., Goh, F., Yang, I. A., 2012. Respiratory health effects of diesel particulate matter. Respirology. https://doi.org/10.1111/j.1440-1843.2011.02109.x.

Roqué, P.J., Dao, K., Costa, L.G., 2016. Microglia mediate diesel exhaust particle-induced cerebellar neuronal toxicity through neuroinflammatory mechanisms. Neurotoxicology 56, 204–214. https://doi.org/10.1016/j.neuro.2016.08.006.

Schraufnagel, D.E., 2020. The health effects of ultrafine particles. Exp. Mol. Med. https://doi.org/10.1038/s12276-020-0403-3.

Schwarze, P.E., Totlandsdal, A.I., Låg, M., Refsnes, M., Holme, J.A., Øvrevik, J., 2013. Inflammation-related effects of diesel engine exhaust particles: Studies on lung cells in vitro. Biomed Res. Int. https://doi.org/10.1155/2013/685142.

Shkirkova, K., Lamorie-Foote, K., Zhang, N., Li, A., Diaz, A., Liu, Q., Thorwald, M.A., Godoy-Lugo, J.A., Ge, B., D'Agostino, C., Zhang, Z., Mack, W.J., Sioutas, C., Finch, C. E., Mack, W.J., Zhang, H., 2022. Neurotoxicity of Diesel Exhaust Particles. J Alzheimers Dis. 89 (4) https://doi.org/10.3233/JAD-220493.

Staal, Y.C.M., Li, Y., Gerber, L.S., Fokkens, P., Cremers, H., Cassee, F.R., Talhout, R., Westerink, R.H.S., Heusinkveld, H.J., 2022. Neuromodulatory and Neurotoxic Effects of e-Cigarette Vapor Using a Realistic Exposure Method. https://doi.org/10.1080/08958378.2022.2118911.

Steiner, S., Czerwinski, J., Comte, P., Müller, L.L., Heeb, N.V., Mayer, A., Petri-Fink, A., Rothen-Rutishauser, B., 2013. Reduction in (pro-)inflammatory responses of lung cells exposed invitro to diesel exhaust treated with a non-catalyzed diesel particle filter. Atmos. Environ. 81, 117–124. https://doi.org/10.1016/j.atmosenv.2013.08.029.

Steiner, S., Czerwinski, J., Comte, P., Heeb, N.V., Mayer, A., Petri-Fink, A., Rothen-Rutishauser, B., 2015. Effects of an iron-based fuel-borne catalyst and a diesel particle filter on exhaust toxicity in lung cells in vitro. Anal. Bioanal. Chem. 407, 5977–5986. https://doi.org/10.1007/s00216-014-7878-5.

Tan, J.H., Shi, X.Y., Zhang, J., He, K.B., Ma, Y.L., Ge, Y.S., Tan, J.W., 2009. Effects of biodiesel on fine particles (PM2.5) and polycyclic aromatic hydrocarbons from diesel engine. Huanjing Kexue/environmental Sci. 30, 2839–2844.

Totlandsdal, A.I., Flemming, C.R., Schwarze, P., Refsnes, M., Låg, M., 2010. Diesel exhaust particles induce CYP1A1 and pro-inflammatory responses via differential pathways in human bronchial epithelial cells. Part. Fibre Toxicol. 7 https://doi.org/10.1186/1743-8977-7-41.

Traviss, N., Thelen, B.A., Ingalls, J.K., Treadwell, M.D., 2010. Biodiesel versus diesel: a pilot study comparing exhaust exposures for employees at a rural municipal facility. J. Air Waste Manag. Assoc. 60, 1026–1033. https://doi.org/10.3155/1047-3289.60.9.1026.

Upadhyay, S., Stoeger, T., Harder, V., Thomas, R.F., Schladweiler, M.C., Semmler-Behnke, M., Takenaka, S., Karg, E., Reitmeir, P., Bader, M., Stampfl, A., Kodavanti, U.P., Schulz, H., 2008. Exposure to ultrafine carbon particles at levels below detectable pulmonary inflammation affects cardiovascular performance in spontaneously hypertensive rats. Part. Fibre Toxicol. 5 https://doi.org/10.1186/1743-8977-5-19.

Valdivia, P., Martin, M., LeFew, W.R., Ross, J., Houck, K.A., Shafer, T.J., 2014. Multi-well microelectrode array recordings detect neuroactivity of ToxCast compounds. Neurotoxicology 44, 204–217. https://doi.org/10.1016/j.neuro.2014.06.012.